COLLÈGE DE FRANCE
1530

Chaire de Physique
de la Matière Condensée
Antoine Georges

Contrôle des fonctionnalités des oxydes

Hétéro-structures, Impulsions Lumineuses

Cours 1 – Introduction Générale

Cycle 2016-2017
25 avril 2017

COLLÈGE DE FRANCE
1530

Chaire de Physique
de la Matière Condensée
Antoine Georges

Control of oxide functionalities:

Heterostructures, Light pulses

Lecture 1 - Overview

Most slides will be in English

2016-2017 Lectures
April 25, 2017

Today's seminar

Jean-Marc Triscone

University of Geneva

Department of Quantum Matter Physics

Interfacial effects and superconductivity in oxide heterostructures

25 avril

Cours : Introduction et vue d'ensemble : contrôle des fonctionnalités des oxydes – interfaces et hétérostructures.

Séminaire : Jean-Marc Triscone (DQMP – Université de Genève)

Interfacial effects and superconductivity in oxide heterostructures

2 mai

Cours : Oxydes, interfaces et héterostructures : de la structure à la structure électronique

Séminaire : Alexandre Gloter et Odile Stephan (LPS, Orsay)

Explorer la physique aux interfaces d'oxydes fortement corrélés : résultats récents et perspectives en microscopie électronique

9 mai

Cours : Les nickelates $RNiO_3$: une transition métal-isolant contrôlable au mécanisme original

Séminaire : Marcelo Rozenberg (LPS, Orsay)

Transition-metal oxides under strong electric fields, from resistive switching to artificial synapses and neurons

16 mai

Cours : Contrôle des degrés de liberté orbitaux dans les nickelates et autres oxydes – vers un supraconducteur « synthétique » ?

Séminaire : Andres Santander-Syro (CSNSM, Orsay)

Novel two-dimensional electron systems at the surface of transition-metal oxides

23 mai

Cours : Ruthénates : compétition entre champ cristallin, couplage spin-orbite et couplage de Hund.

Séminaire : Darrell Schlom (Cornell University)

Thin Film Alchemy: Using Epitaxial Engineering to Unleash the Hidden Properties of Oxides

30 mai

Cours : Contrôle par impulsions lumineuses – vue d'ensemble et « phononique non-linéaire ».

Séminaire : Manuel Bibes (CNRS-Thales)

Electric-field control of magnetism in oxide heterostructures

Today’s lecture is a broad, non-technical overview

Disclaimer: This is a very broad field which has undergone fast development in the last ~ 15 years.
A quick search reveals several ~1000 published articles
This set of lectures is merely a glimpse into some aspects of the field.

OXIDES:
Old
and
New

Rust: oxyde/hydroxide.
(wikipedia)

$La_{2-x}Sr_xCuO_4$

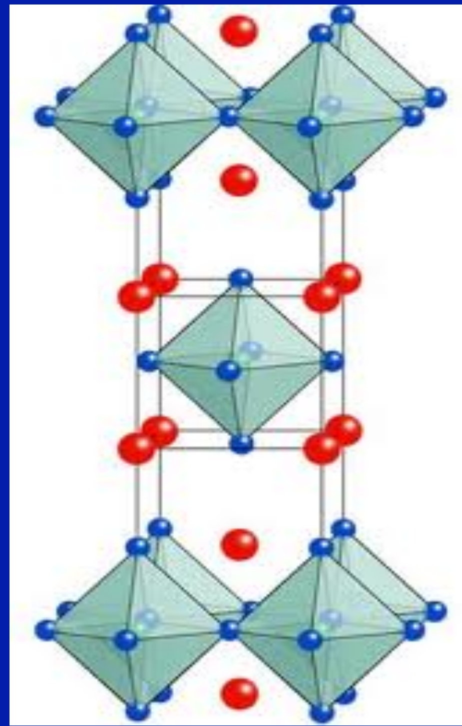

« Artificial materials »
Molecular Beam
Epitaxy (MBE)
allows for
synthesis one atomic
layer at a time

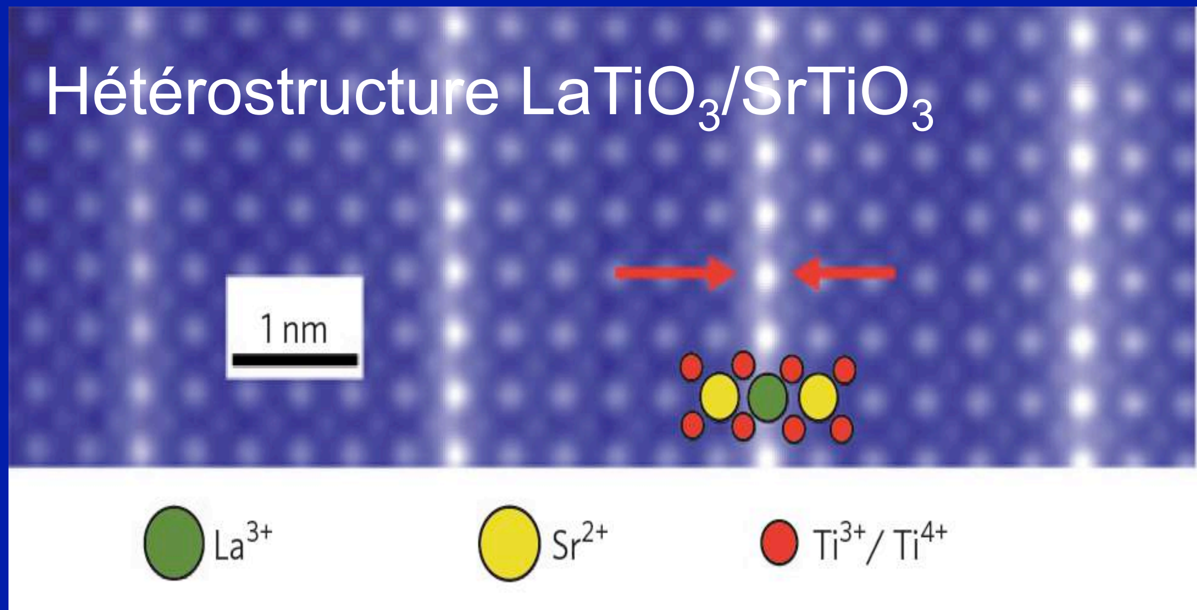

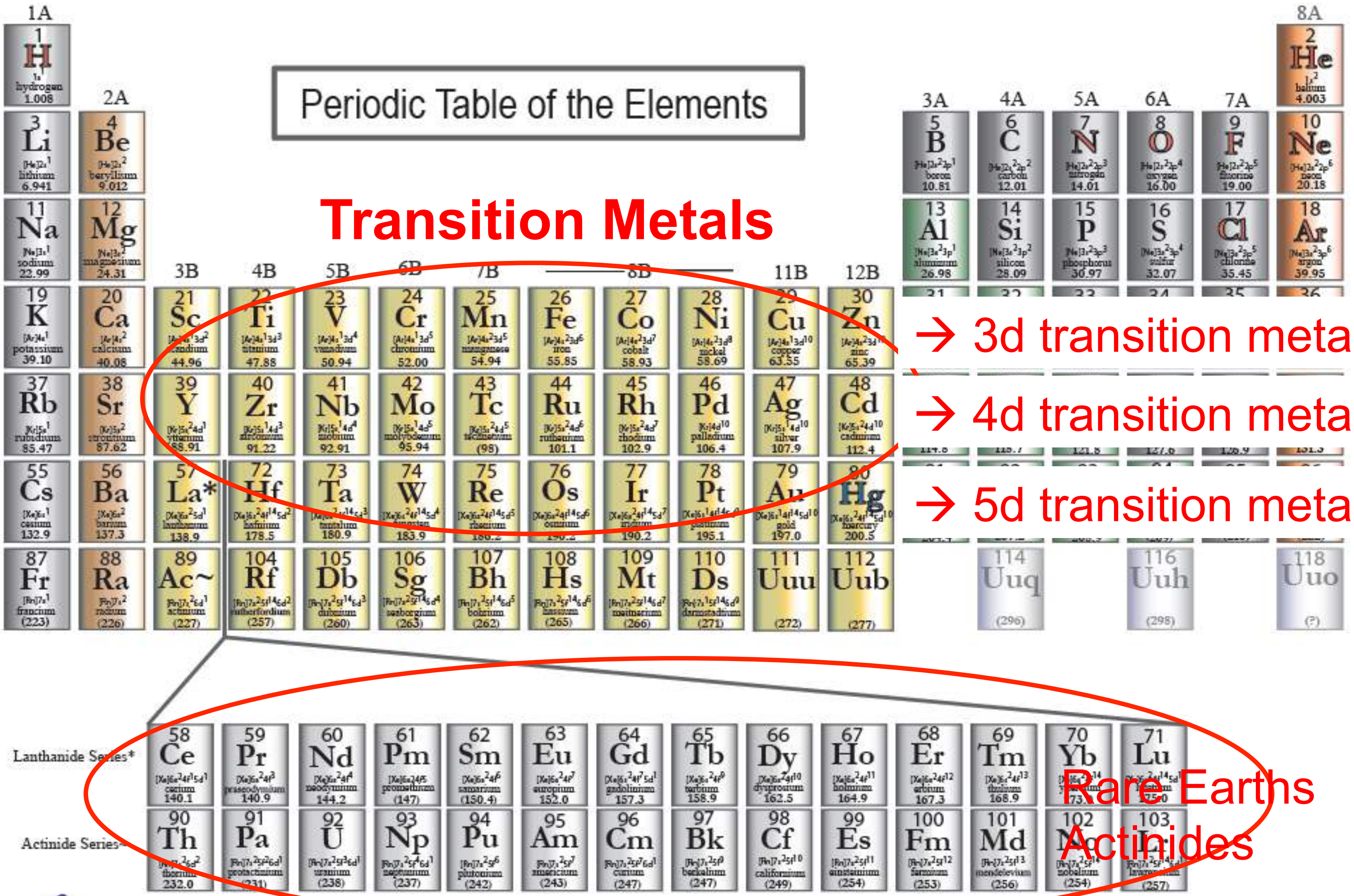

Transition Metals

→ 3d transition metals

→ 4d transition metals

→ 5d transition metals

Rare Earths

Actinides

Oxides (especially those with strong electron correlations/partially filled shells) do "BIG THINGS"

- Because of the strong interdependence of electrons, collective phenomena take place
- Such as: metal-insulator transitions, magnetism, superconductivity, etc.
- → Interesting functionalities
- → Fundamental questions in physics and chemistry

Metal-Insulator Transitions

Metal-Insulator Transitions:

V_2O_3 : a time-honored example displaying a rich variety of phenomena

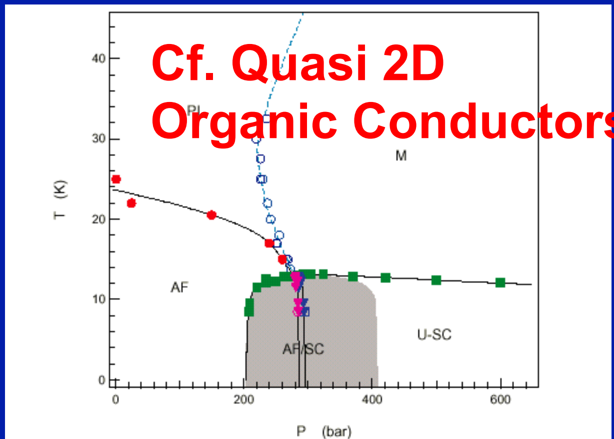

FIG. 1. Temperature *vs* pressure phase diagram of κ−Cl. The antiferromagnetic (AF) critical line $T_N(P)$ (dark circles) was determined from NMR relaxation rate while $T_c(P)$ for unconventional superconductivity (U-SC: squares) and the metal-insulator $T_{MI}(P)$ (MI: open circles) lines were obtained from the AC susceptibility. The AF-SC boundary (double dashed line) is determined from the inflexion point of $\chi'(P)$ and, for 8.5K, from sublattice magnetization. This boundary line separates two regions of inhomogeneous phase coexistence (shaded area).

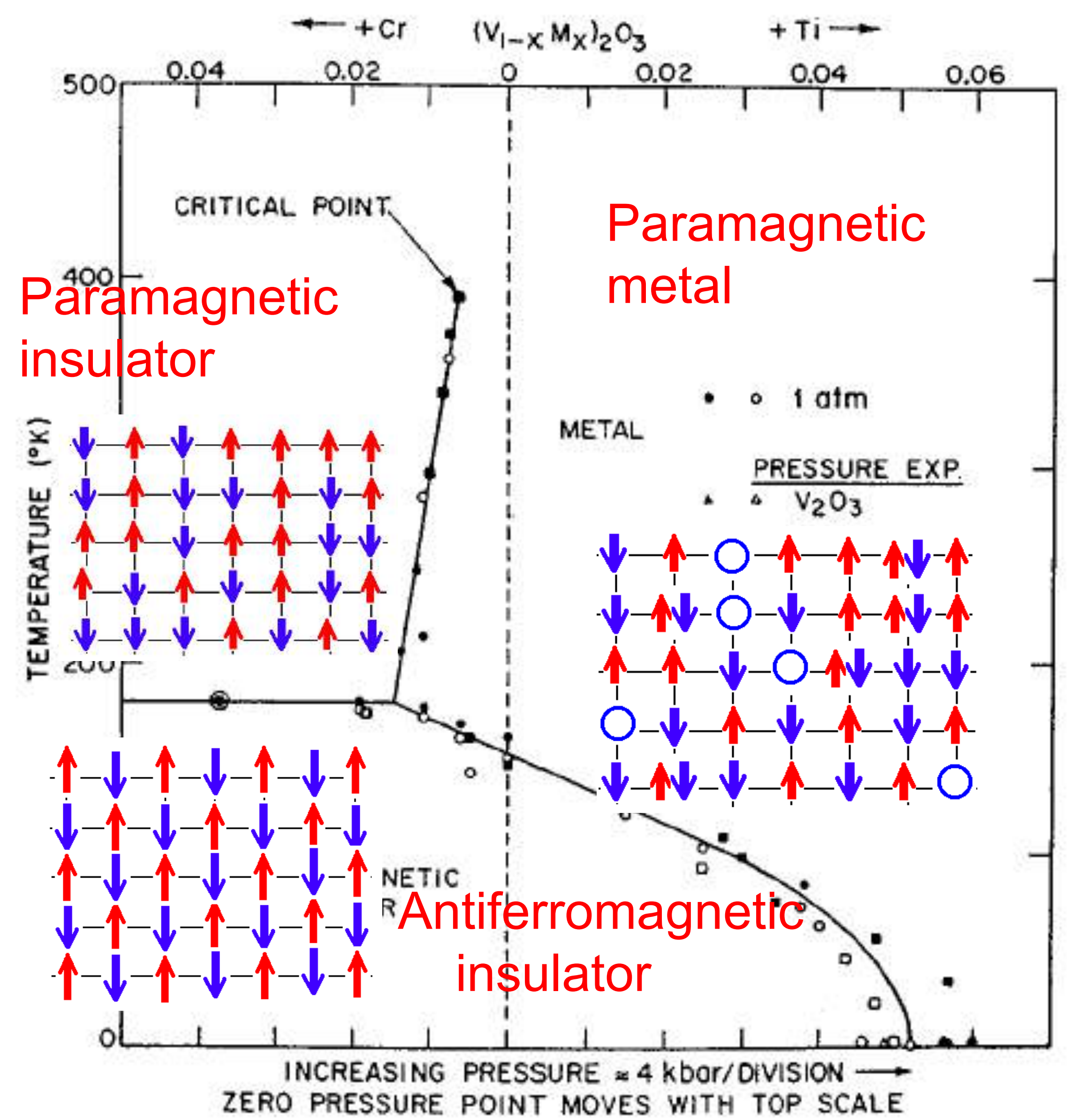

FIG. 70. Phase diagram for doped V_2O_3 systems, $(V_{1-x}Cr_x)_2O_3$ and $(V_{1-x}Ti_x)_2O_3$. From McWhan *et al.*, 1971, 1973.

Rare-Earth Nickelates $RNiO_3$: Tunable MIT

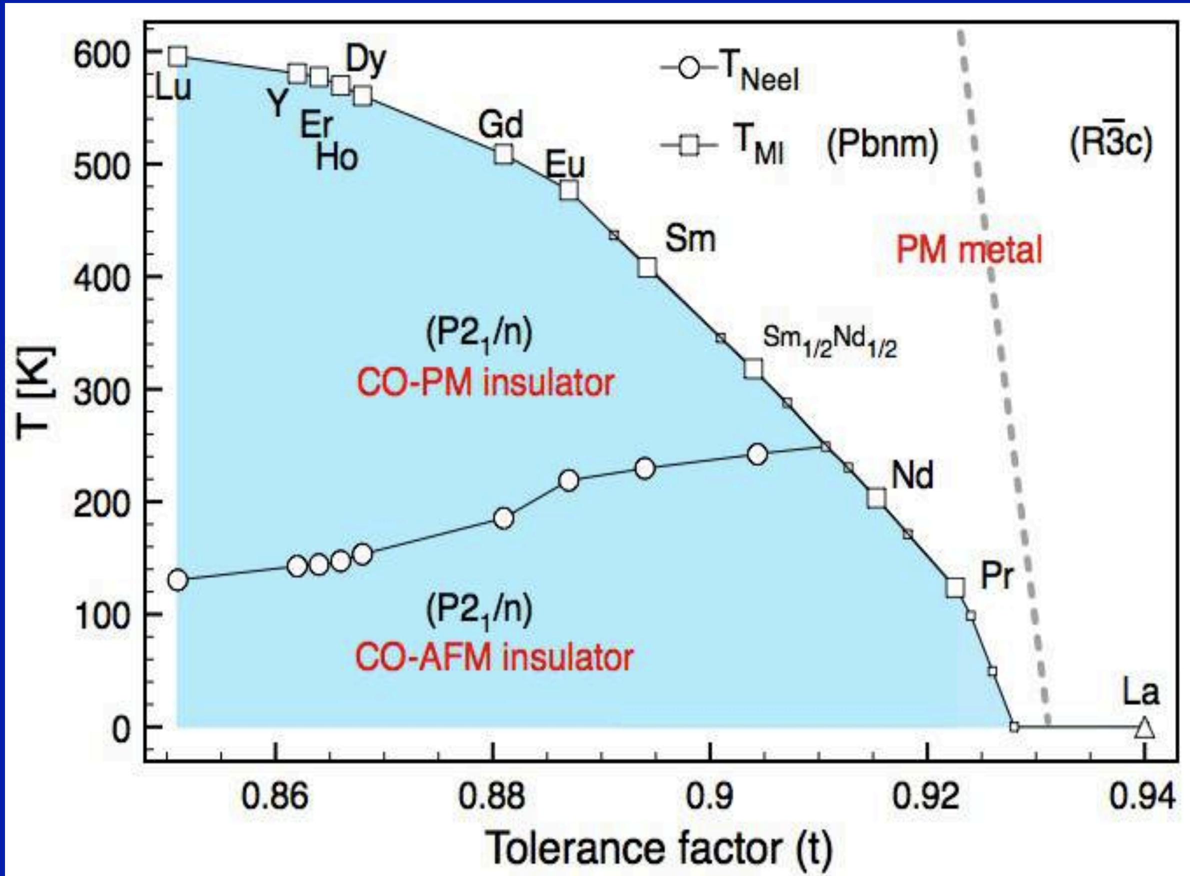

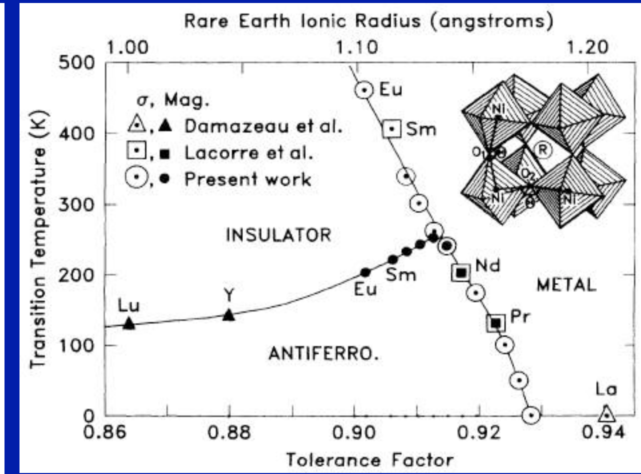

$$t = \frac{d_{\mathrm{R-O}}}{\sqrt{2}d_{\mathrm{Ni-O}}}$$

Tolerance factor:
smaller t
= Larger distortion

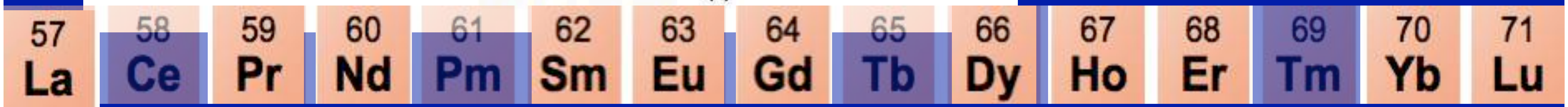

R.Sherwitzl, PhD thesis, Geneva 2012 Adapted from Catalan, *Phase Transitions*, (2008)

Early work: Demazeau et al. (Bordeaux, Hagenmuller's group 1971) Lacorre, Torrance et al. 1992 (IBM San Jose & Le Mans)

Magnetism, Charge Ordering and “Colossal” Magnetoresistance: Manganites

Manganites – Multiple Electronic Phases and ``Colossal Magnetoresistance''

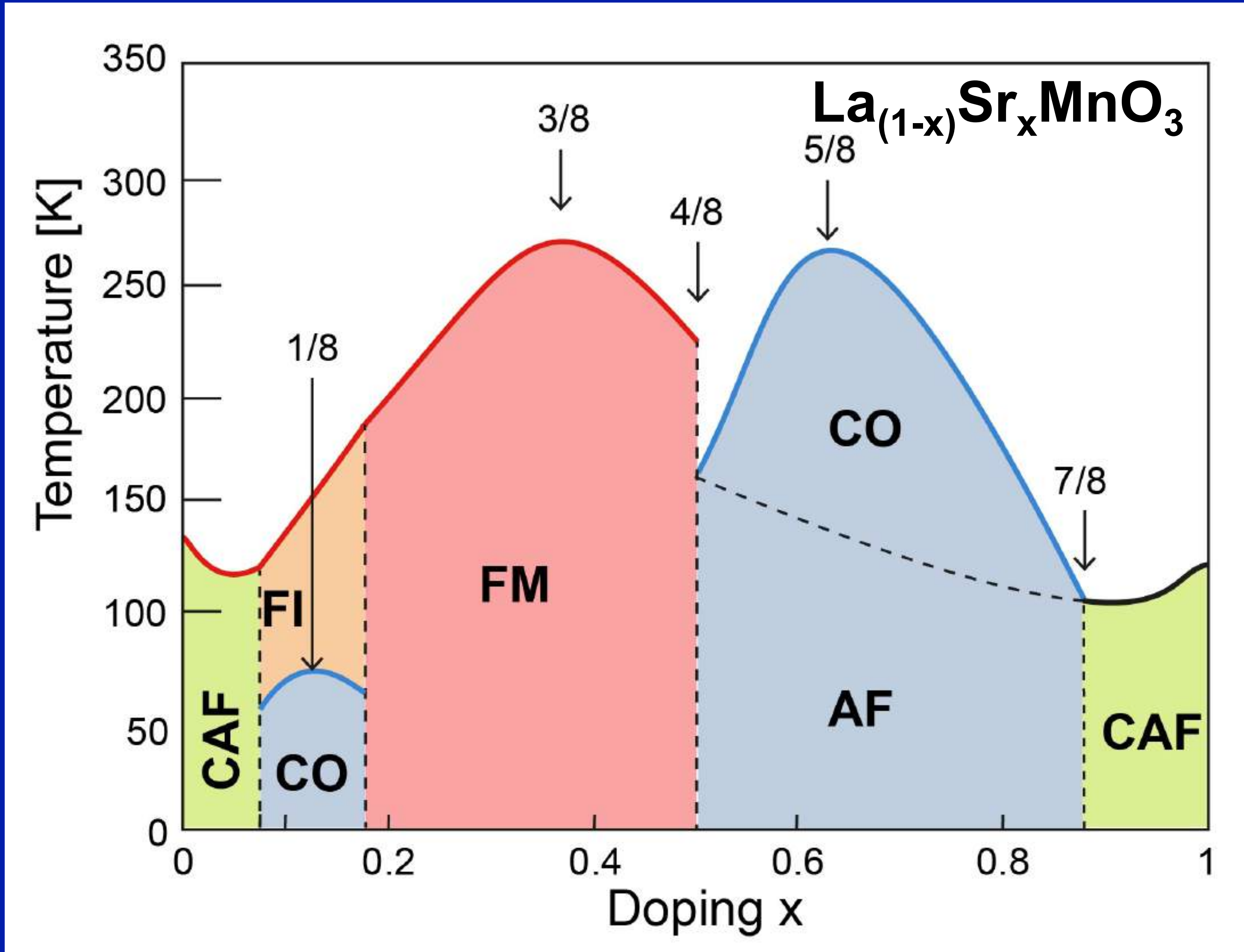

Ferroelectricity

- Prototypical example: perovskite oxide $BaTiO_3$

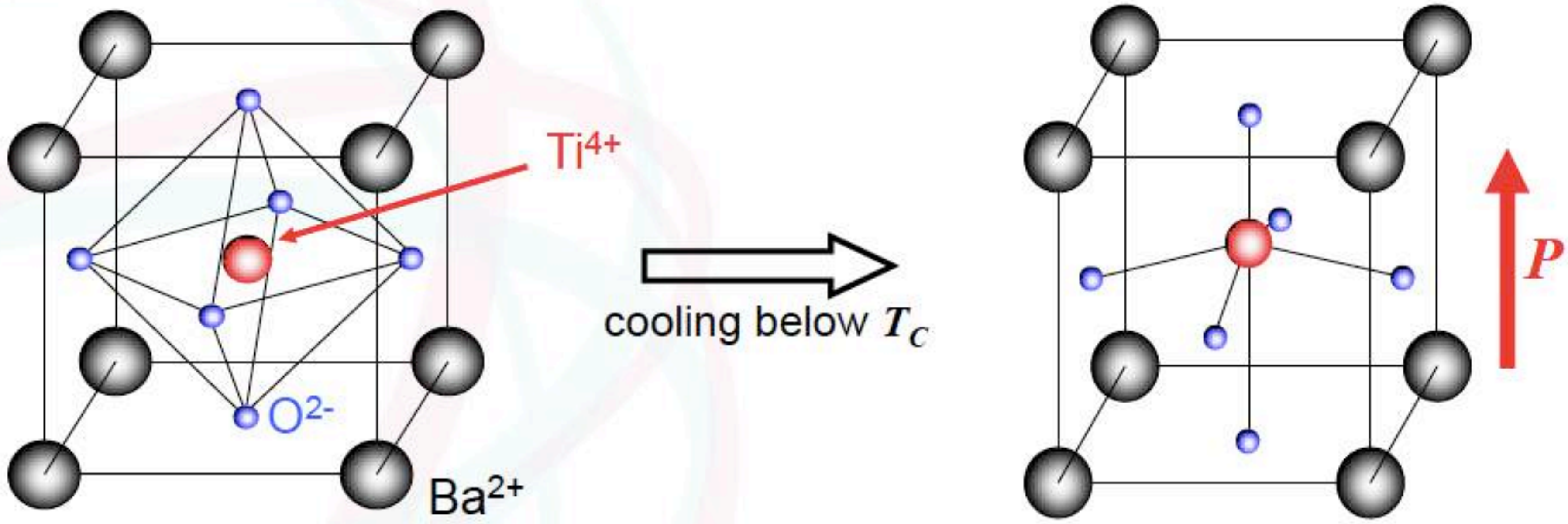

Paraelectric phase

Ferroelectric phase

- In ferroelectric phase: "center of mass" of positive charges is displaced with respect to "center of mass" of negative charges

- As a result, **spontaneous polarization P appears**

Ferroelectricity + Magnetism: *Multiferroics*

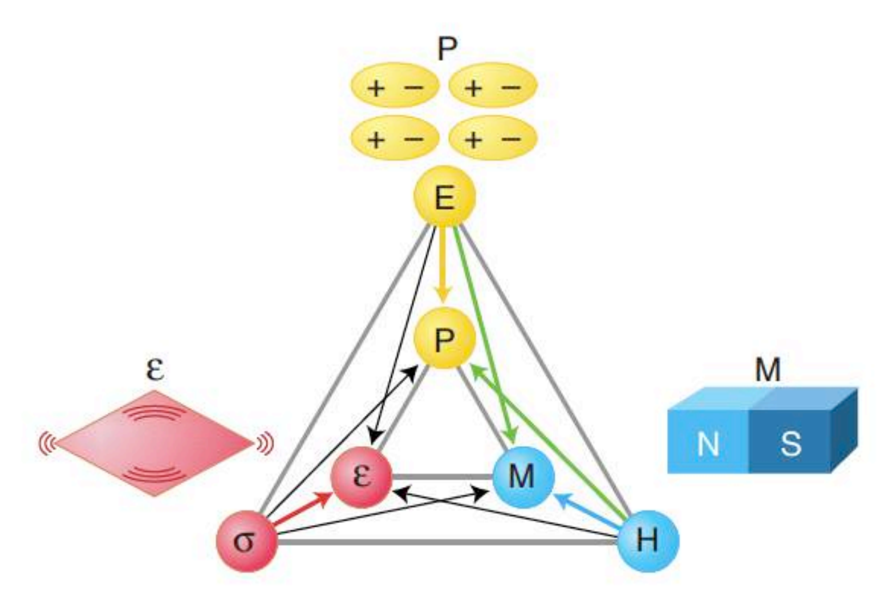

Phase control in ferroics and multiferroics. The electric field E, magnetic field H, and stress σ control the electric polarization P, magnetization M, and strain ε, respectively. In a ferroic material, P, M, or ε are spontaneously formed to produce ferromagnetism, ferroelectricity, or ferroelasticity, respectively. In a multiferroic, the coexistence of at least two ferroic forms of ordering leads to additional interactions. In a magnetoelectric multiferroic, a magnetic field may control P or an electric field may control M (green arrows).

N.Spaldin, Science, 2005

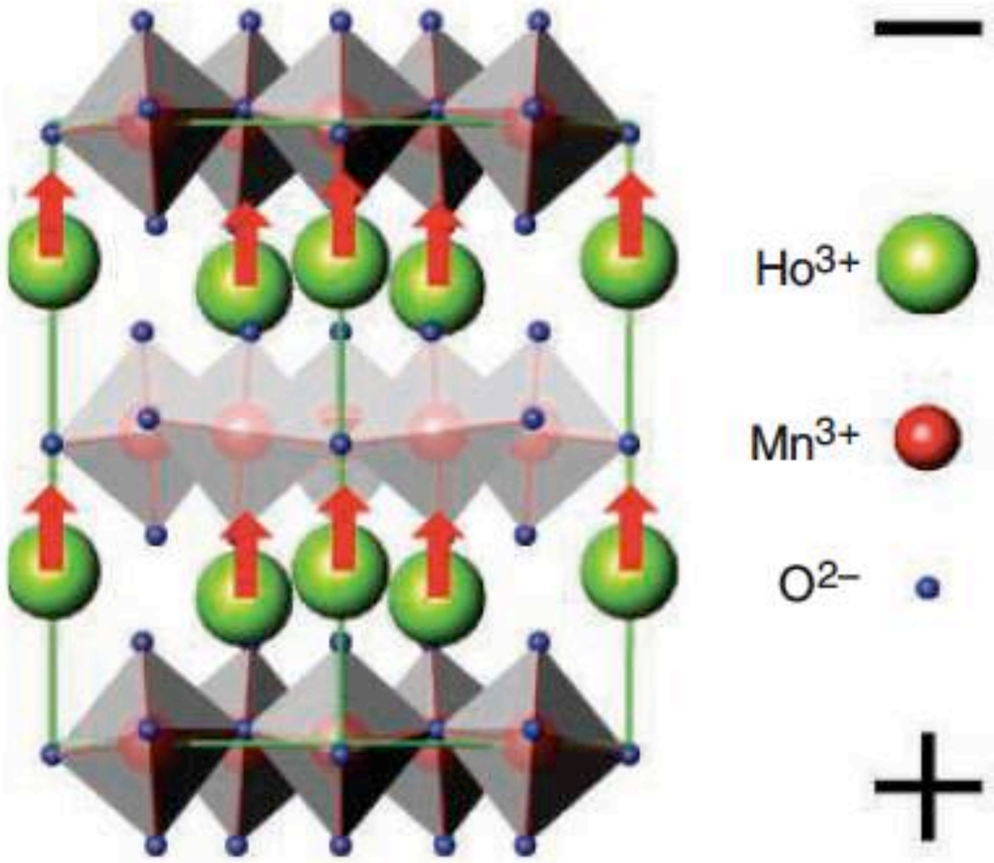

Structure of multiferroic $HoMnO_3$. Hexagonal $HoMnO_3$ is ferroelectric, because the oxygen bipyramids surrounding each Mn^{3+} ion are tilted and shifted relative to the Ho^{3+} ions. It is also magnetic, with ferromagnetic alignment of the Ho^{3+} magnetic moments combined with antiferromagnetic Mn^{3+} ordering. Therefore, hexagonal $HoMnO_3$ is multiferroic.

Thermoelectric performance of some oxides

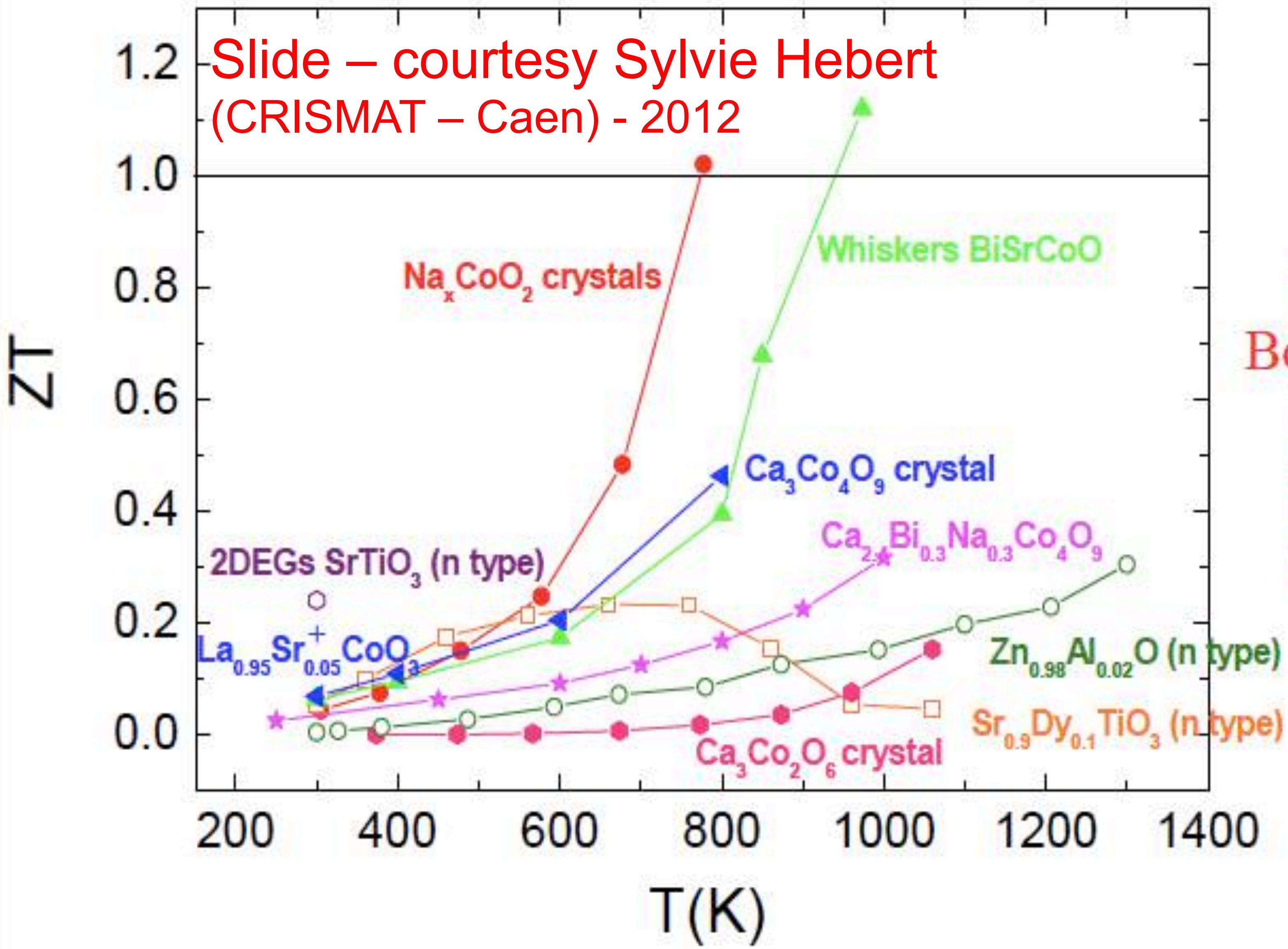

Oxydes :
Bonne stabilité
chimique
à haute T
et sous air

NaxCoO2 _ Fujita : JJAP 40, 4644 (2001); SrTiO3 _ Muta : J. Alloys and compounds 350, 292 (2003); Ca2.4Bi0.3Na0.3Co4O9 _ Xu : APL80, 3760 (2002); Whiskers BiSrCoO _ Funahashi : APL81, 1459 (2002); Ca3Co2O6 _ Mikami : JAP94, 10 (2003); 2DEGs(SrTiO3) _ Ohta : Nature Materials 6, 129 (2007); Ca3Co4O9 crystal _ Shikano : APL 82, 1851 (2003); LaSrCoO _ Androulakis : APL84, 1099 (2004); ZnAlO _ Ohtaki : JAP79, 1816 (1996)

“High-Temperature” Superconductivity : Cuprates

Copper-oxide « High-Tc » Superconductors

The Nobel Prize in Physics 1987

"for their important break-through in the discovery of superconductivity in ceramic materials"

K.A. Müller

J.G. Bednorz

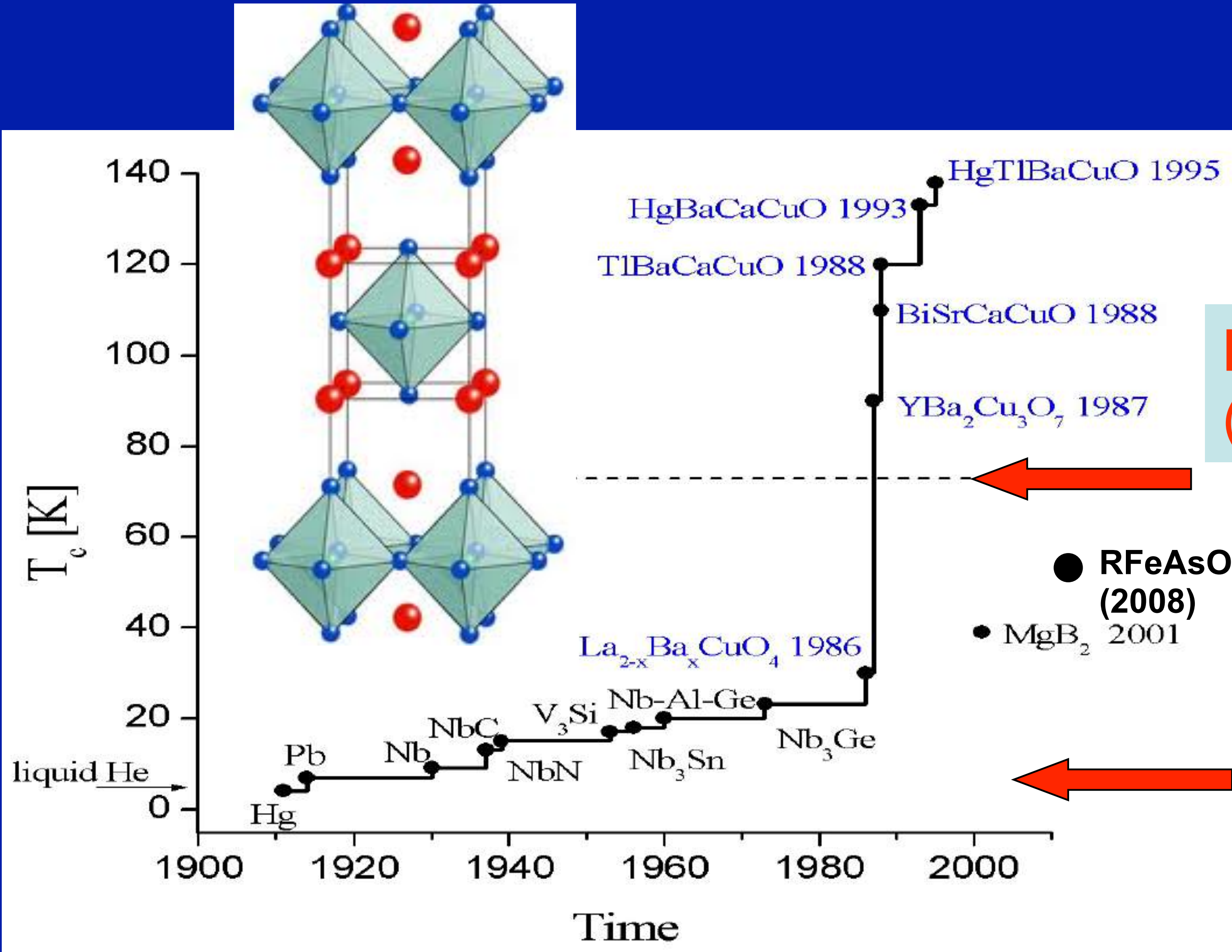

Liquid Nitrogen (77 K)

Liquid Helium (4 K)

Copper-oxide superconductors:

Rich phase diagram with mysterious electronic phases

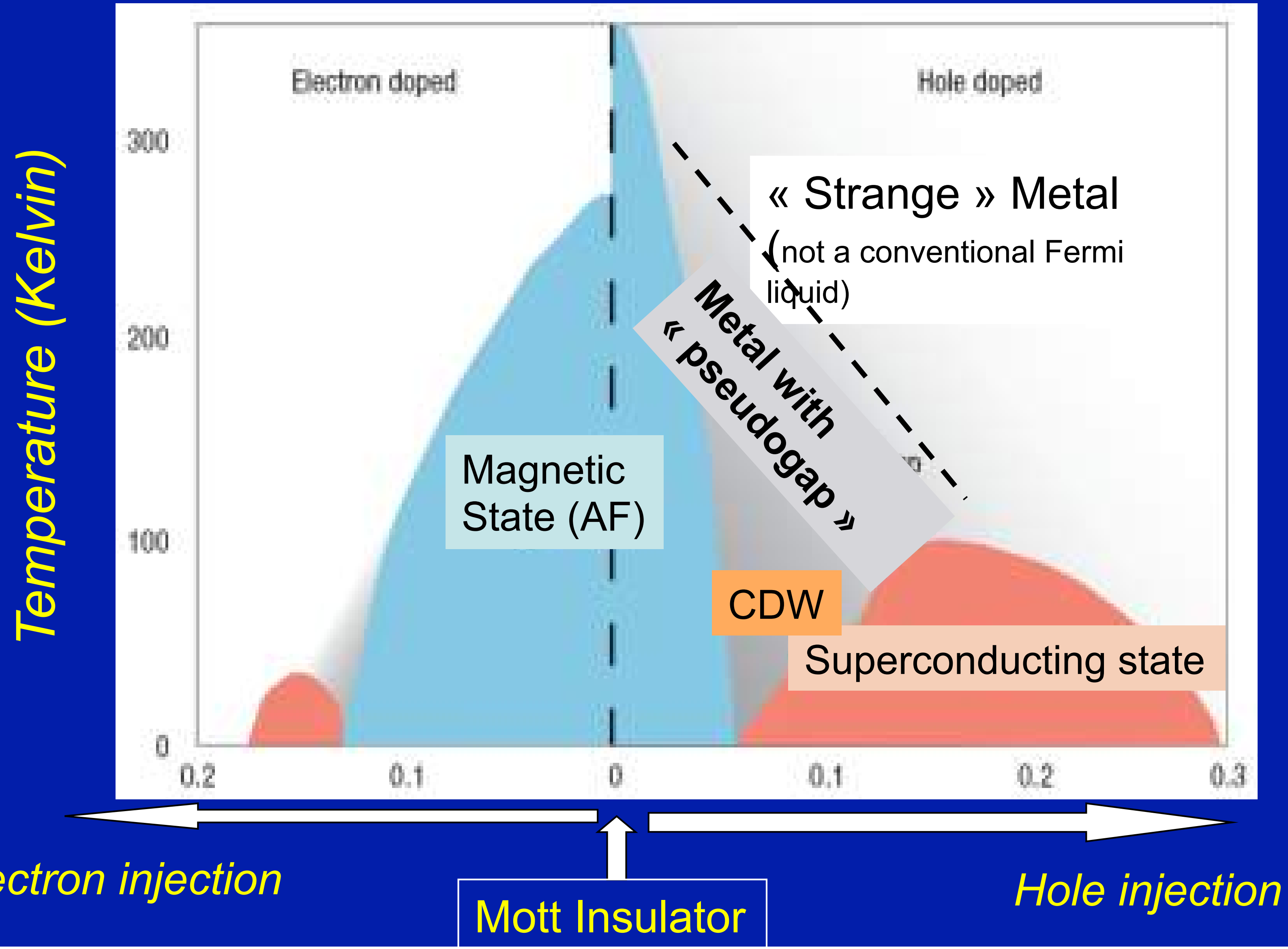

These phase diagrams tell us that:

- Many possible phases compete
- Presumably: small energy differences between them
- Both a blessing and a challenge for CONTROL !
- Control parameters in the bulk: Chemical composition (with or without injecting charge carriers/changing valence of metal ion/Doping), Pressure, etc.

Can we `teach' correlated quantum materials to do what we want them to: SELECTIVE CONTROL of structure (and electronic structure) ?

"Frontiers in Quantum Materials Control"
ERC-Synergy project QMAC
A.Cavalleri, A.G., D.Jaksch, J.M. Triscone

http://www.mpsd.mpg.de/48916/Q-MAC-start

European Research Council

CONTROL: Traditional and Novel routes

Bandwidth	Pressure Size of rare-earth Distortion Tolerance factor 3d,4d,5d metal	Strained thin films and heterostructures Light/non-linear phononics
Crystal field, Orbital degeneracy	Size of rare-earth Distortion Tolerance factor	- Same -
Filling of shell	Chemistry	Ionic liquids Gating
Doping	Sr,Ca^{2+} → La, RE^{3+}	
Interaction strength	3d,4d,5d metal	Tunable dielectric gating ? Light ?
Charge-Transfer	Change apical oxygen distance Change ligand: O→ S, Se…	Light ?

Two new routes to control

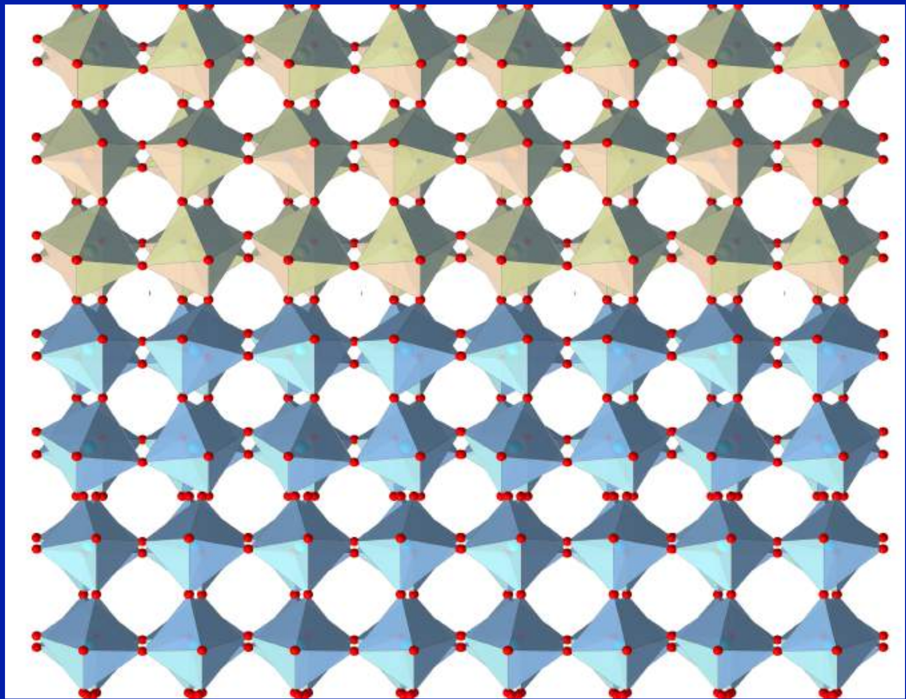

Artificial Materials:
Strained films and
Heterostructures
"Oxytronics/Mottronics"

Selective control with LIGHT

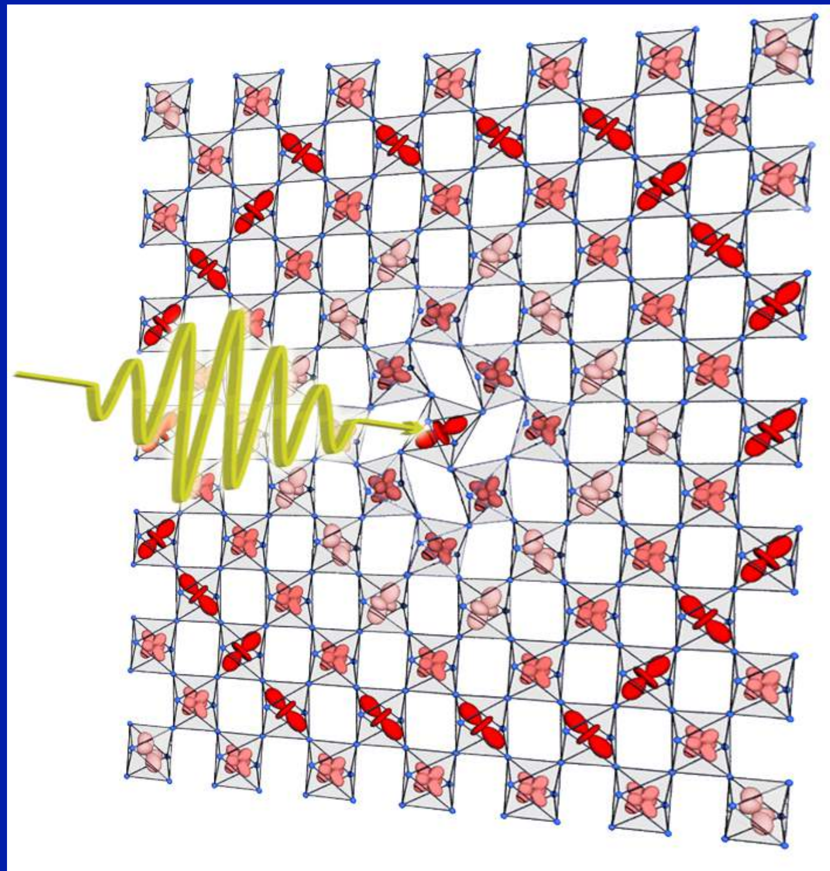

Thin Films and Heterostructures : Materials Elaboration Techniques

- Sputtering (`Pulvérisation cathodique')
- Pulsed Laser Deposition
- Molecular Beam Epitaxy

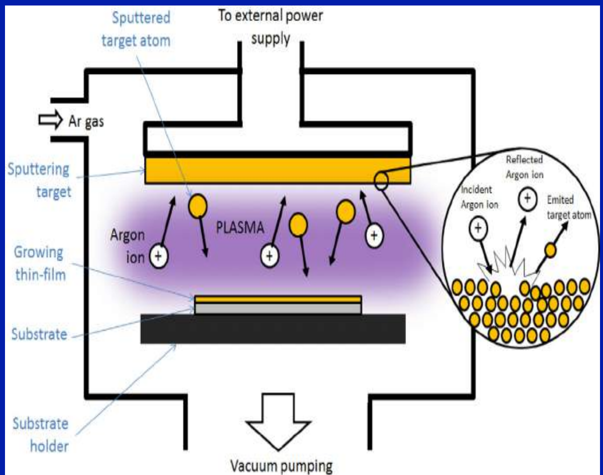

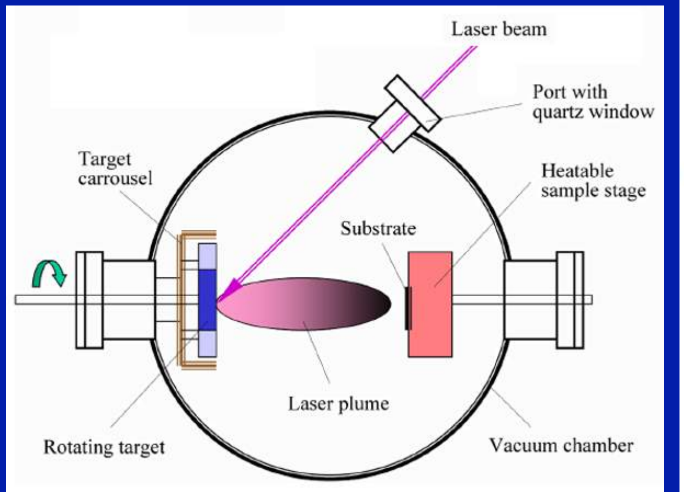

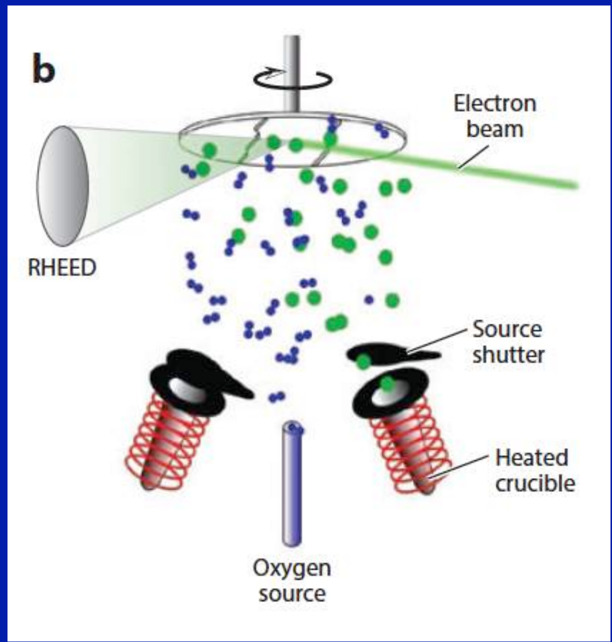

Sputtering (Pulvérisation cathodique)

Image: Pessoa et al.

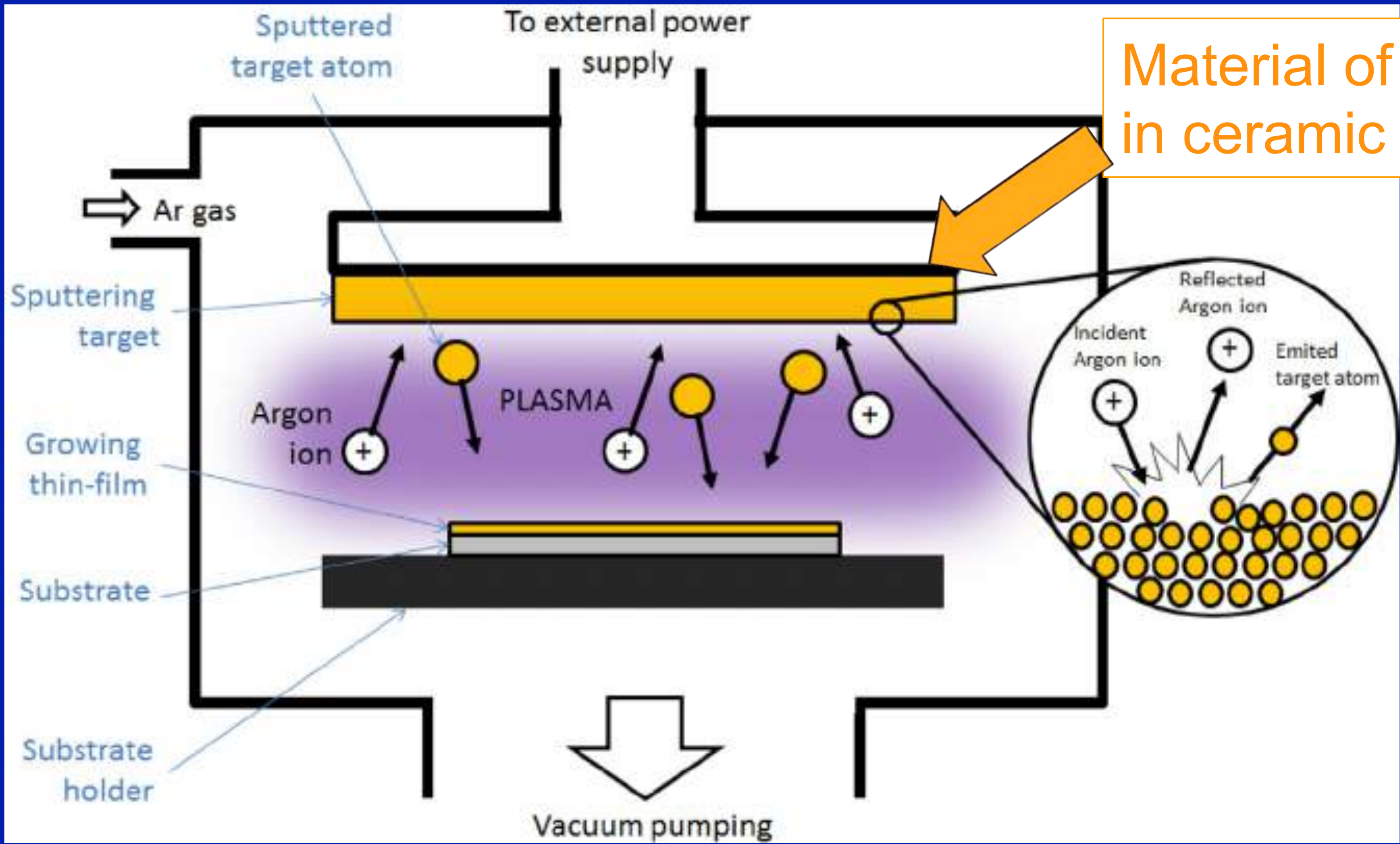

Material of interest, in ceramic form

→ Better control of stoichiometry by off-axis geometry

Pulsed Laser Deposition (PLD)

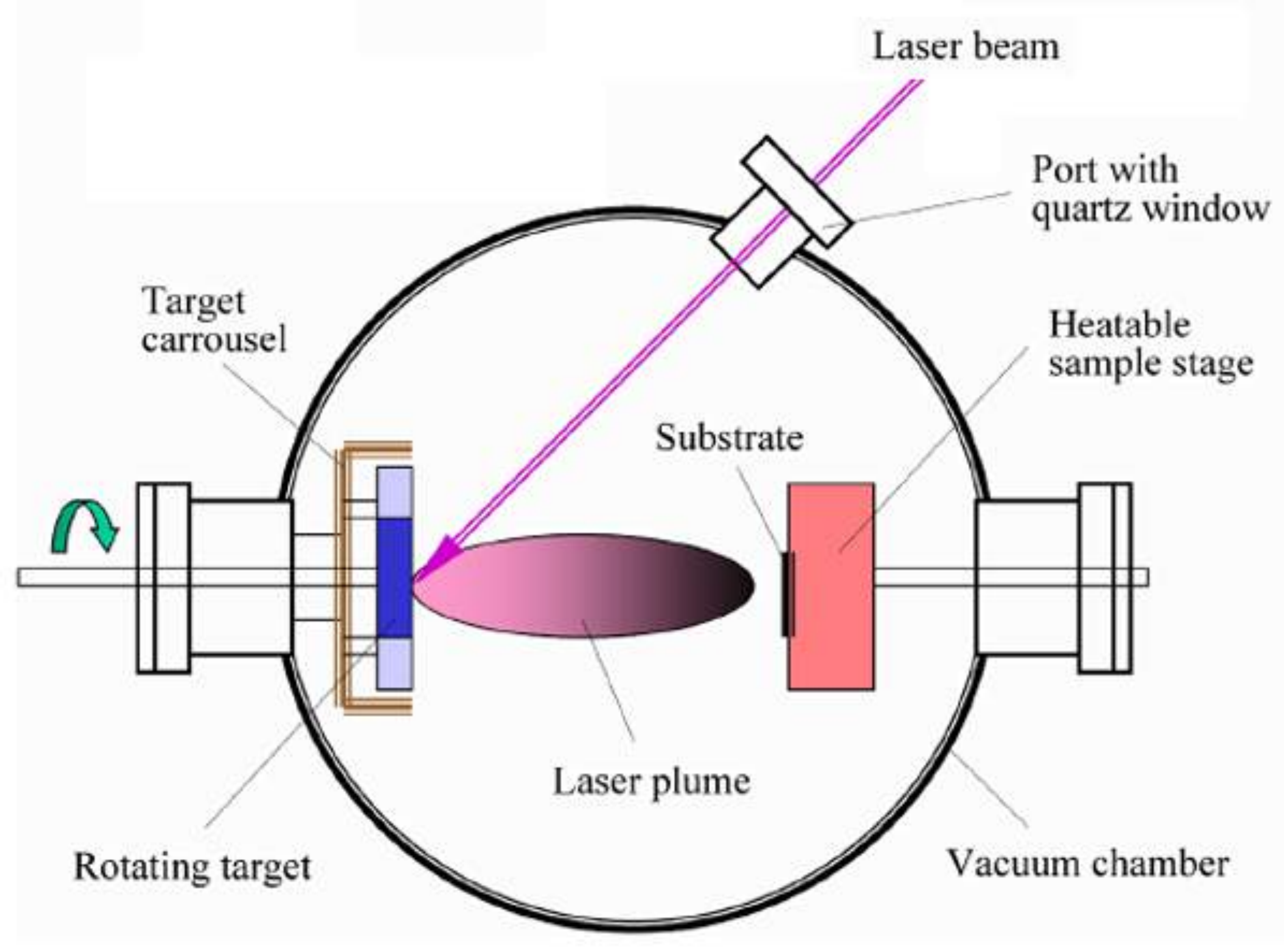

http://groups.ist.utl.pt/rschwarz/rschwarzgroup_files/PLD_files/PLD.htm

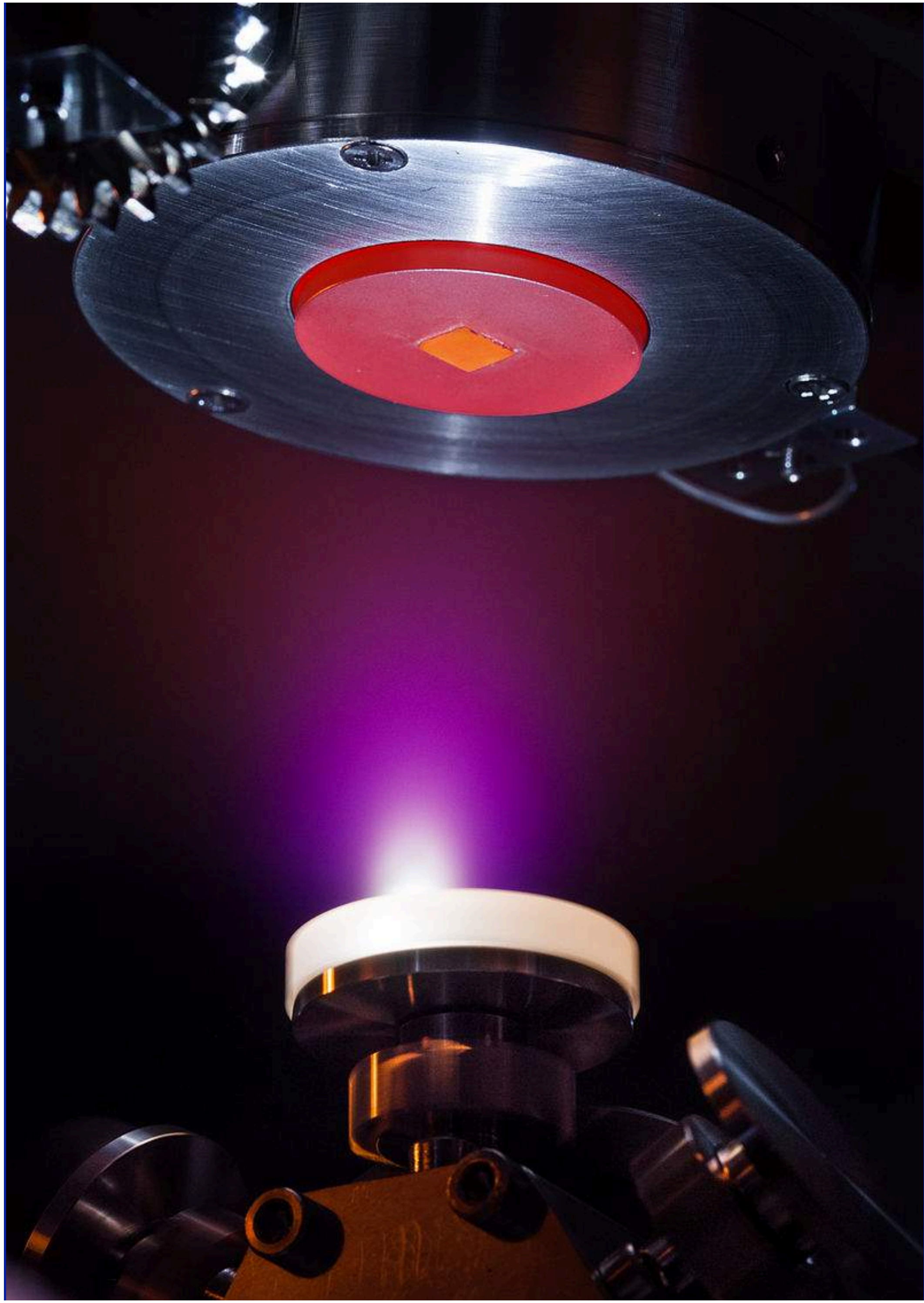

PLD in action

(wikipedia)

Red: heating plate (650 C)

Orange: SrTiO3 substrate (sample)

Plasma plume

Rotating white disk : Al_2O_3

Molecular Beam Epitaxy (MBE)

(Invented@ Bell Labs, 1960's)

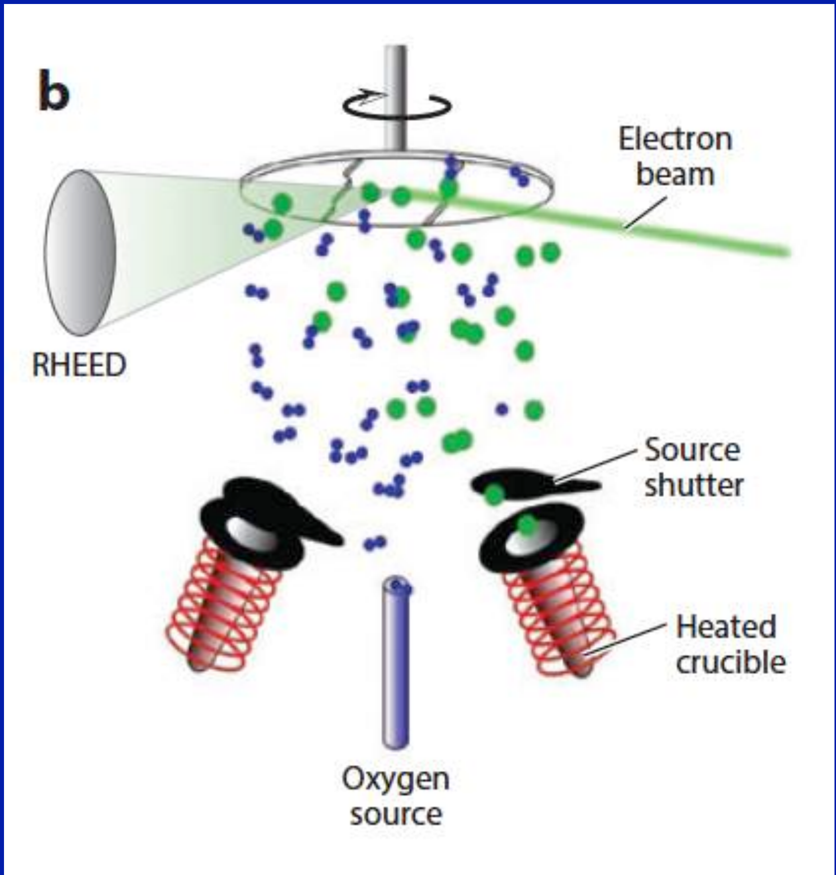

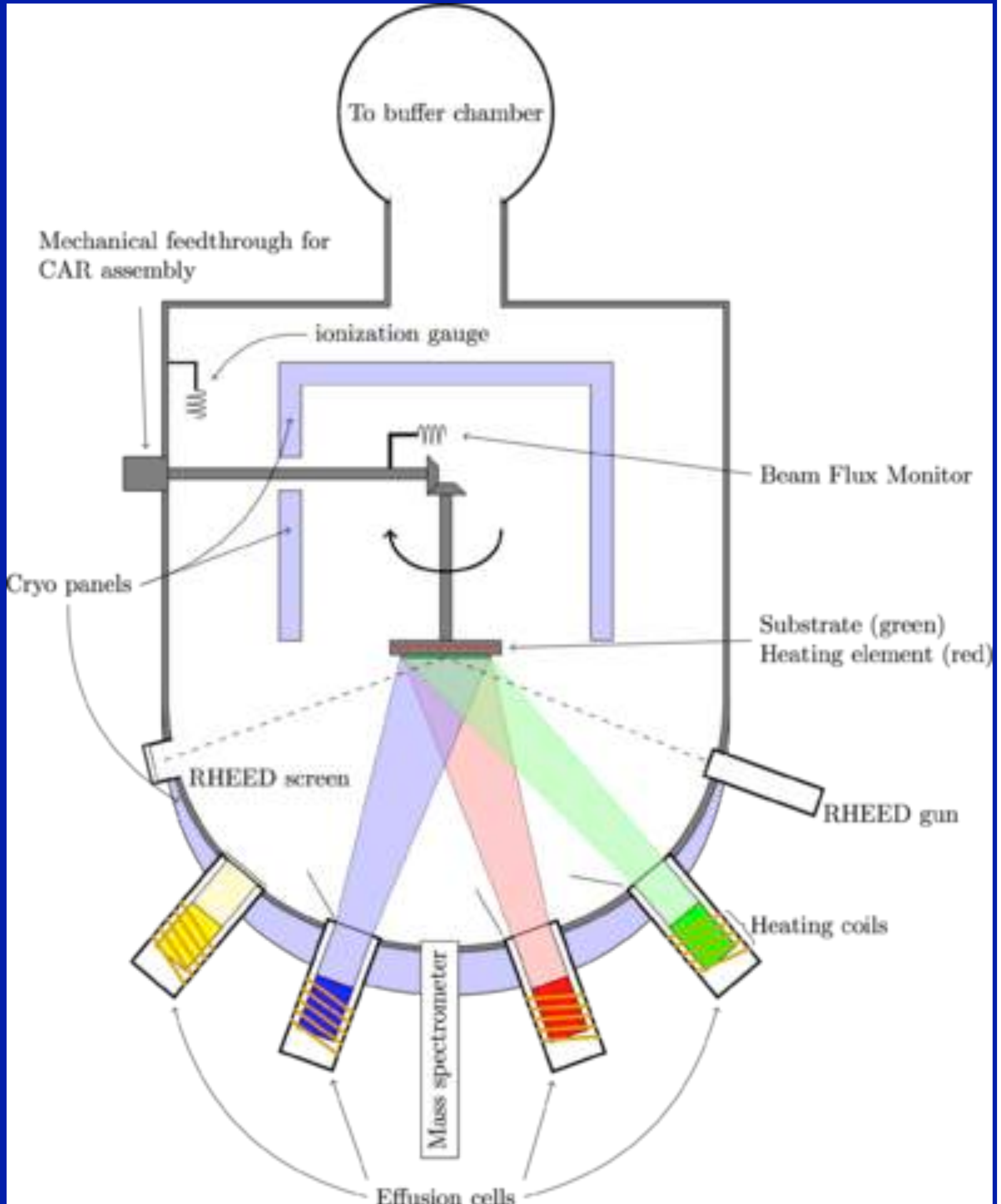

View on the Oxide MBE growth chamber. On the left side: electronic cabinets with power supplys for the effusion cells and e-gun evaporator. In the background: computers for writing recipies for the MBE and for controlling the growth conditions (RGA and RHEED)

Oxide MBE growth chamber
@Jochen Mannart's group – Max Planck Stuttgart (MPI-FKF)

Comparing growth techniques

Sputtering:

+ Easy to implement, flexible

- No in-situ structural/morphology control

PLD (also MBE):

Fast, in-situ RHEED* monitoring possible

(*) Reflection High-Energy Electron Diffraction

MBE:

+ More flexibility in the materials design (atom by atom, layer by layer): does not require a ceramic sample of the material.

Discussion with Jean-Marc Triscone gratefully acknowledged

Quality currently comparable to usual semiconductors

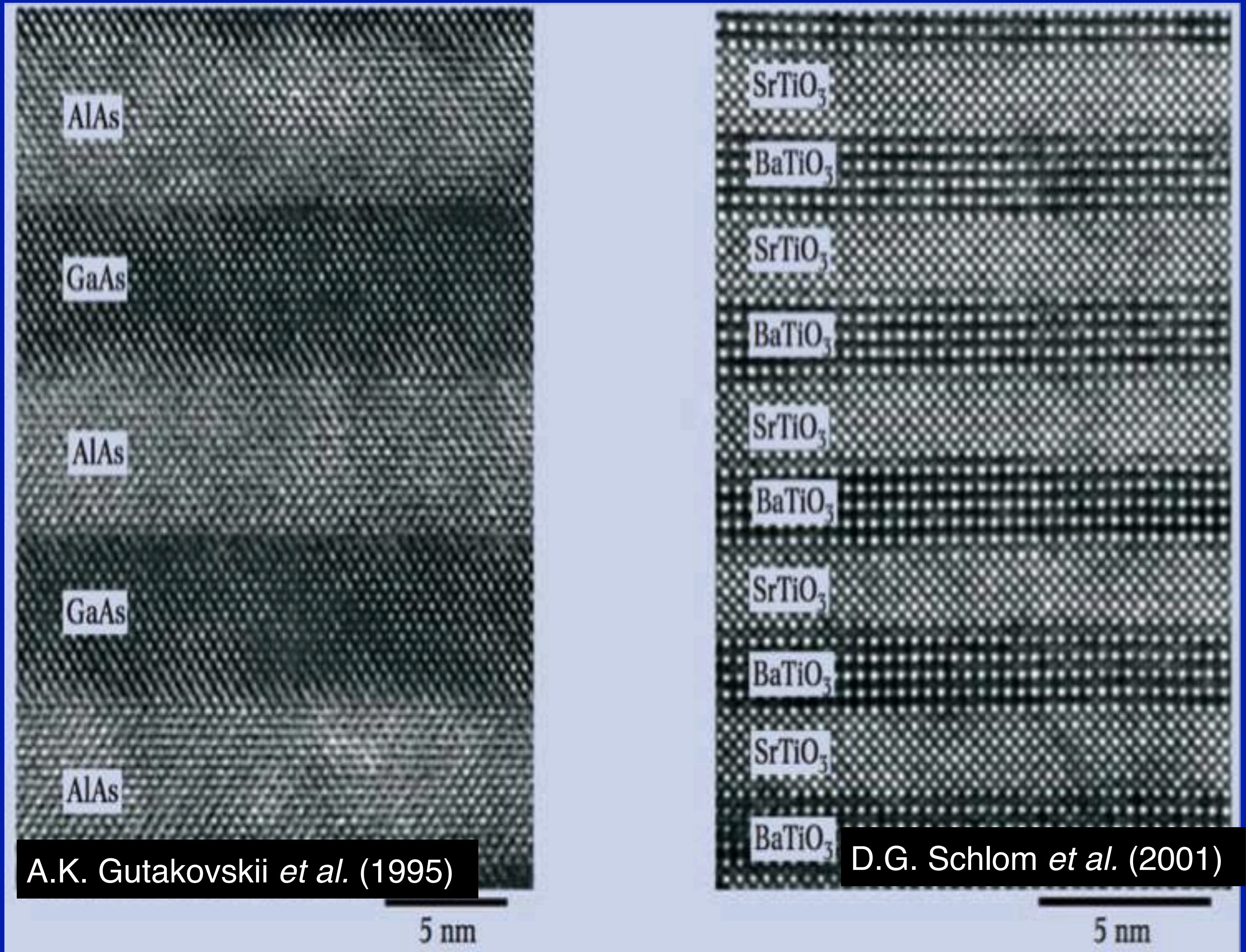

For a review (and many nice pictures) see e.g. Boschker and Mannhart, Annu. Rev. Cond. Mat Phys. 2017

One of the pioneering early works

letters to nature

Nature 419, 378 (2002)

Artificial charge-modulation in atomic-scale perovskite titanate superlattices

A. Ohtomo, D. A. Muller, J. L. Grazul & H. Y. Hwang

Bell Laboratories, Lucent Technologies, Murray Hill, New Jersey 07974, USA

STEM image of a monolayer $LaTiO_3$ embedded in $SrTiO_3$ (1-5 superlattice) PLD grown.

Hwang et al. Nature Mat 11 103 (2012)

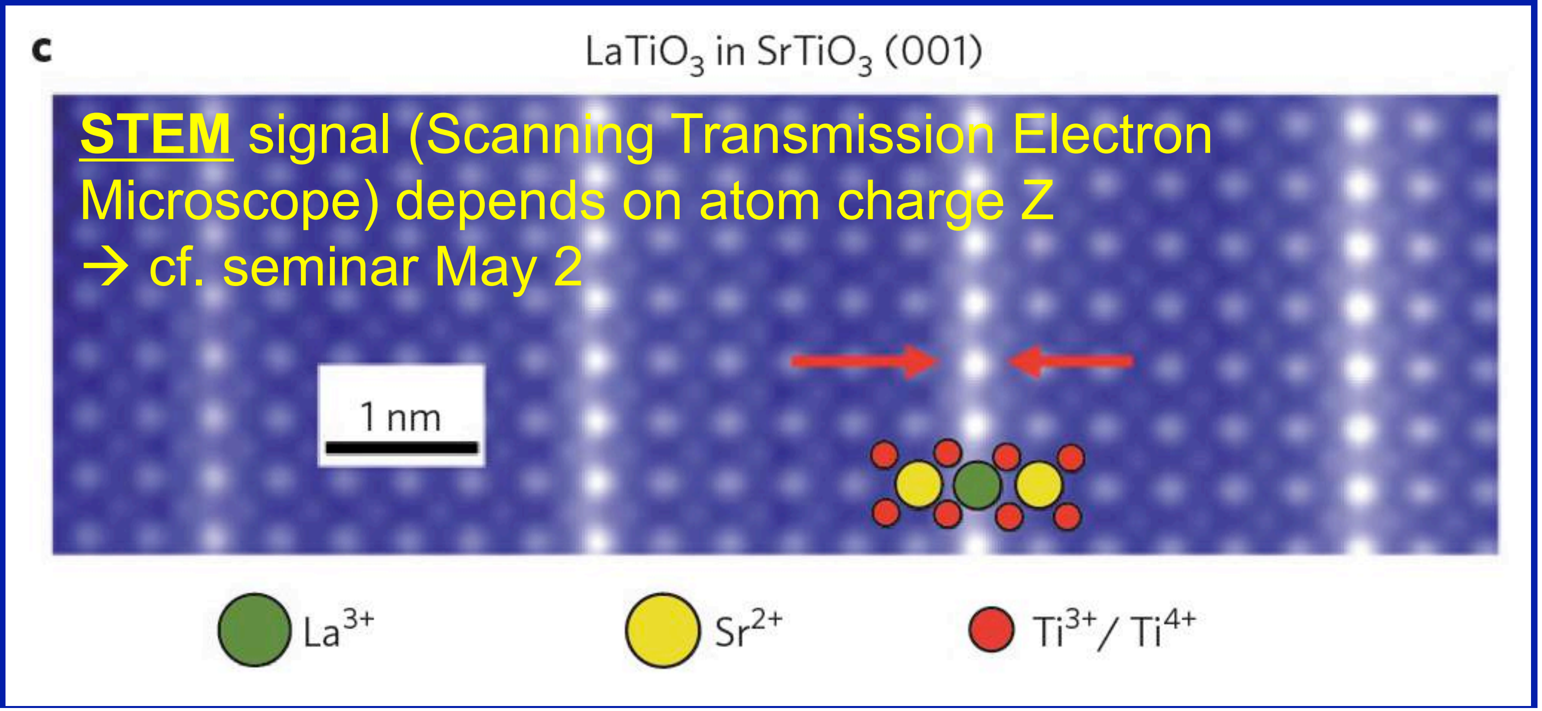

`Epitaxy'

- `επι' = 'above'
- ταξιζ = 'an ordered manner'

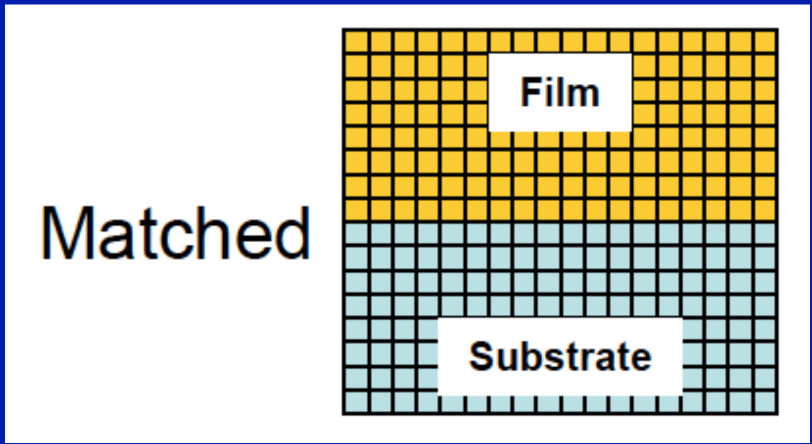

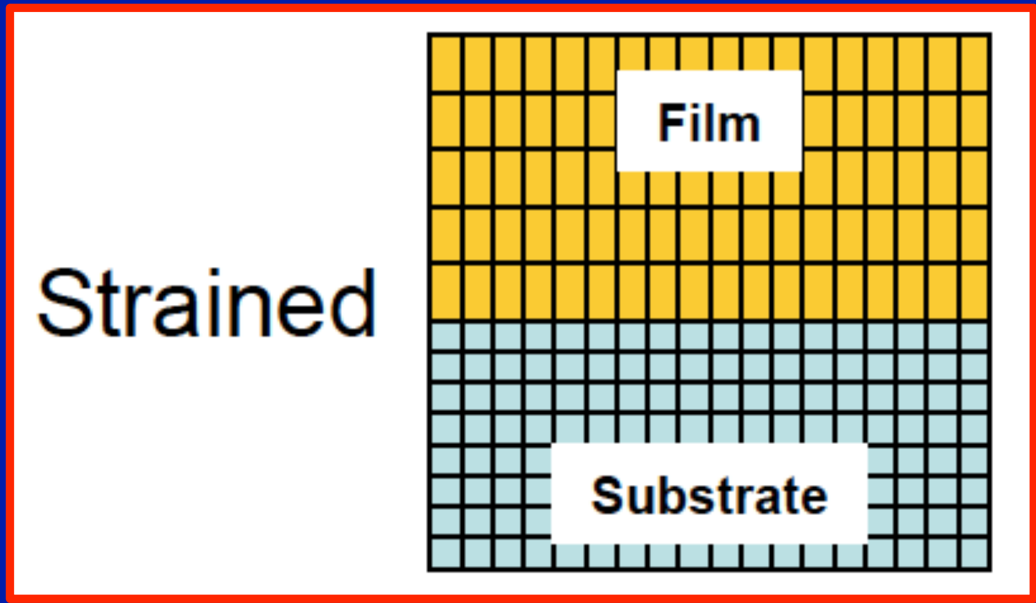

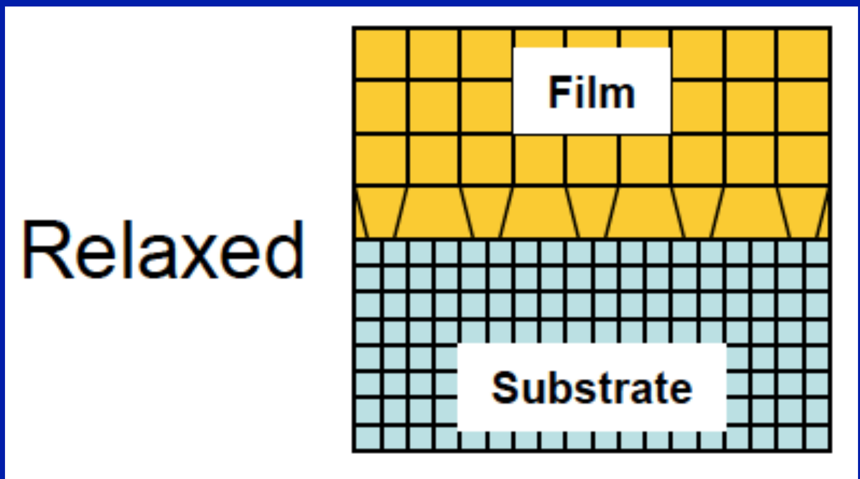

Experimental Probes

- Many of the usual experimental probes in the bulk can be used for thin-films and heterostructures
- e.g. transport, optics, etc…
- But not all !
- Probes that require large amount of matter are a problem: e.g. neutrons. However: neutron reflectometry is sometimes possible
- For buried interfaces, direct access is also an issue.

Surface-sensitive probes
are at home here…

- e.g. (Angular– Resolved) Photoemission Spectroscopy – ARPES
- Can be combined with in-situ MBE growth
- → cf. seminars by A.Santander-Syro, D.Schlom

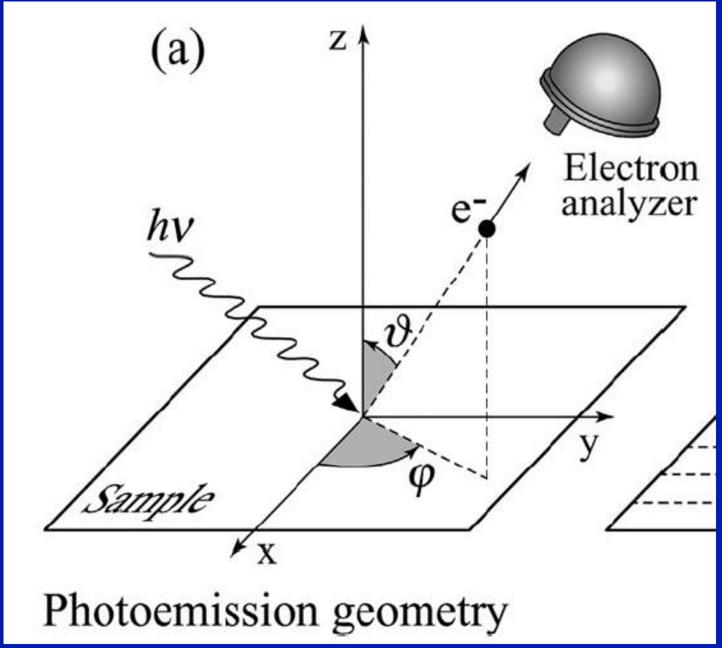

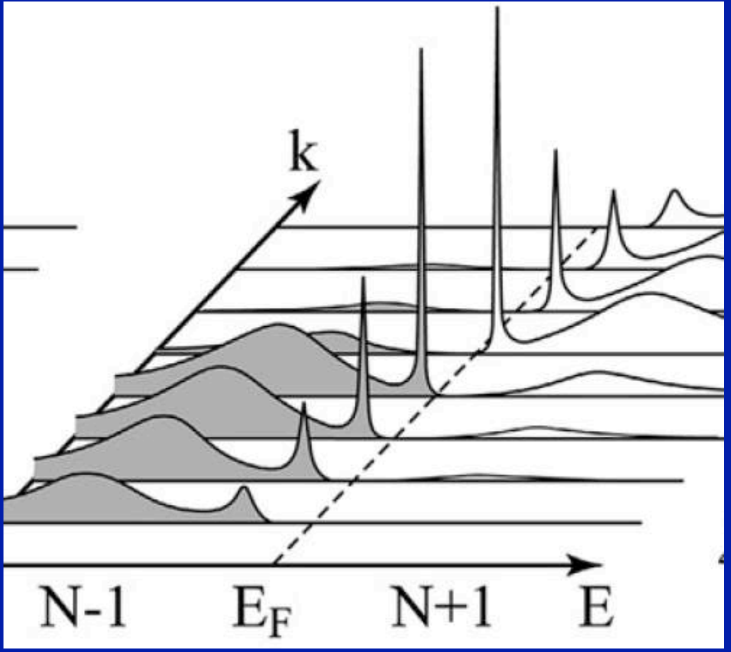

Damascelli, Physica Scripta 2004

PRL **104**, 147601 (2010) PHYSICAL REVIEW LETTERS week ending 9 APRIL 2010

Dimensional-Crossover-Driven Metal-Insulator Transition in $SrVO_3$ Ultrathin Films

K. Yoshimatsu,[1] T. Okabe,[1] H. Kumigashira,[1,2,3,*] S. Okamoto,[4] S. Aizaki,[5] A. Fujimori,[5] and M. Oshima[1,3,6]

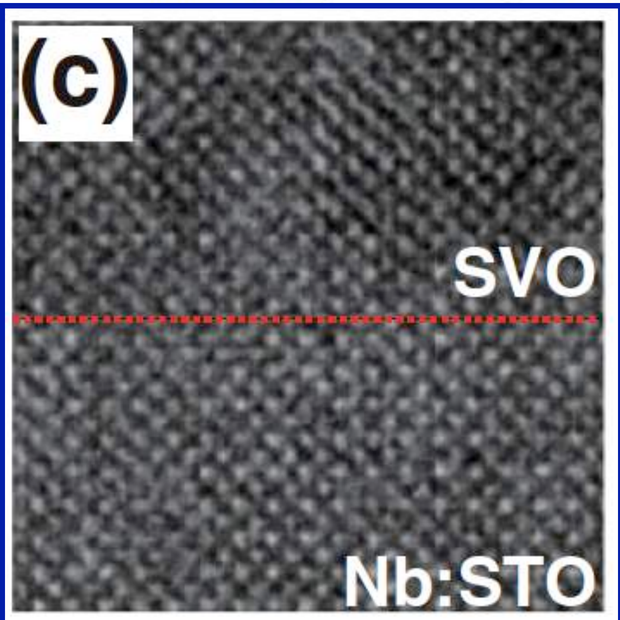

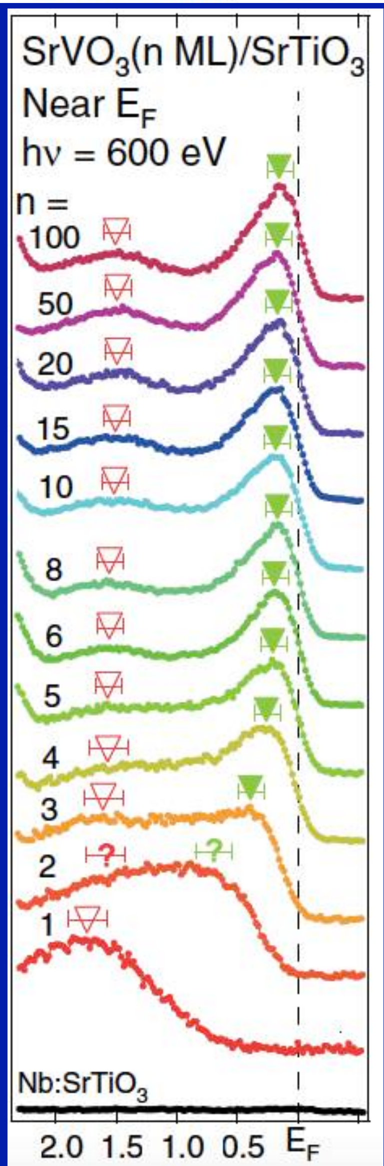

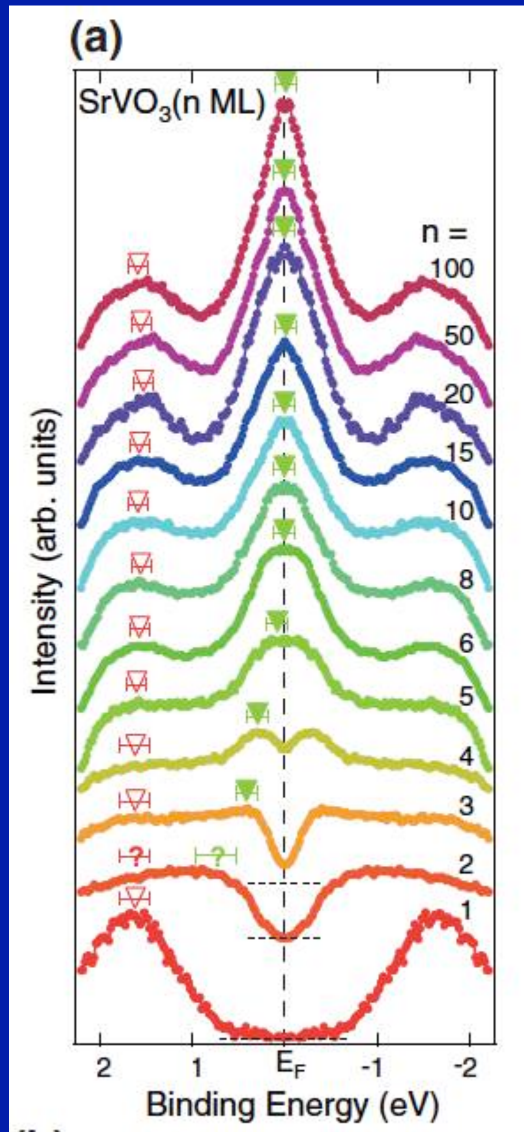

$SrVO_3$ is metallic
in the bulk
These data
reveal a critical thickness
below which
films are insulating

High-resolution probes using synchrotron radiation can probe local structure and electronic structure

- X-ray absorption spectroscopy XAS (possibly with polarized light → sensitivity to orbital occupancies)
- Resonant Inelastic X-ray Scattering (RIXS)
- → The basic principles of these probes will be briefly explained when results are displayed later in the lectures (e.g lectures 3-4 on Nickelates)

RIXS-ID32 spectrometer @ ESRF

Resolution few tens of meV !

A new high resolution soft X-ray RIXS spectrometer has been installed aiming at a combined resolving power $E/\Delta E = 30000$. The spectrometer features an 11m long scattering arm capable of rotating over 100° without breaking vacuum, and a full in-vacuum 4-circle sample goniometer. The instrument was designed and developed in collaboration with Giacomo Ghiringhelli & Lucio Braicovich from Politecnico di Milano.

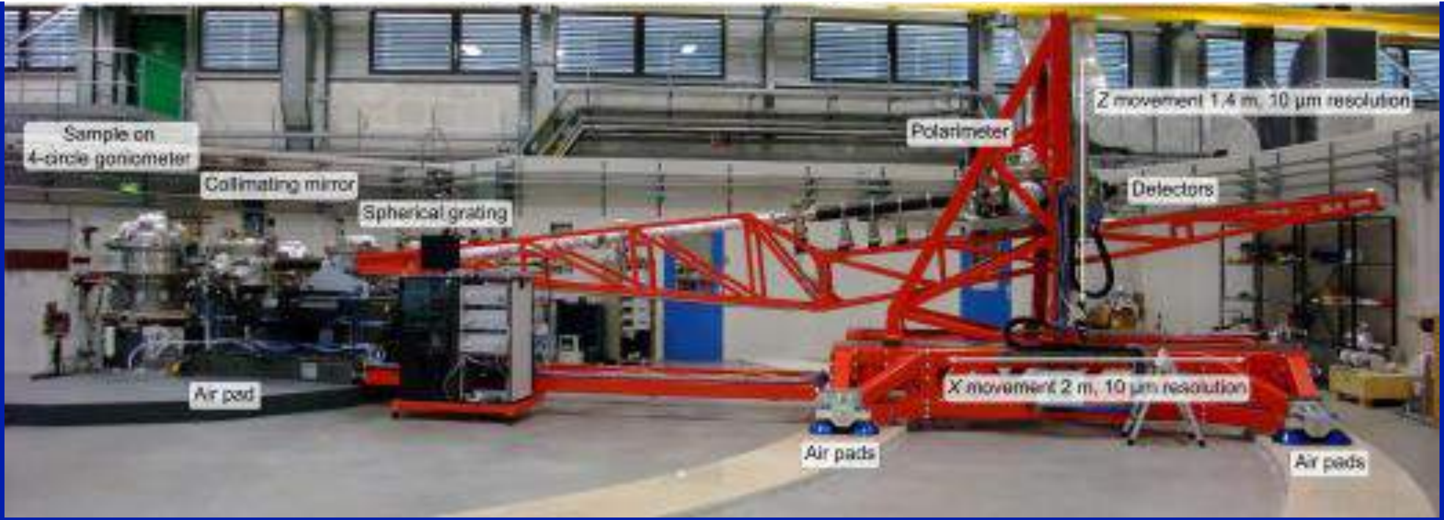

http://www.esrf.eu/home/UsersAndScience/Experiments/EMD/ID32/RIXS.html

Including a movie on how the spectrometer works…

Scanning Transmission Electron Microscopy (STEM) and related techniques (EELS)

→ See seminar on May 2nd (O.Stephan, A.Gloter)

- Scattering amplitude depends strongly on atomic number Z → identify atomic species locally
- In the best cases, these techniques also allow to obtain refined structural information such as local tilts and rotations of MO_6 octahedra (which as we shall see crucially influence electronic properties)

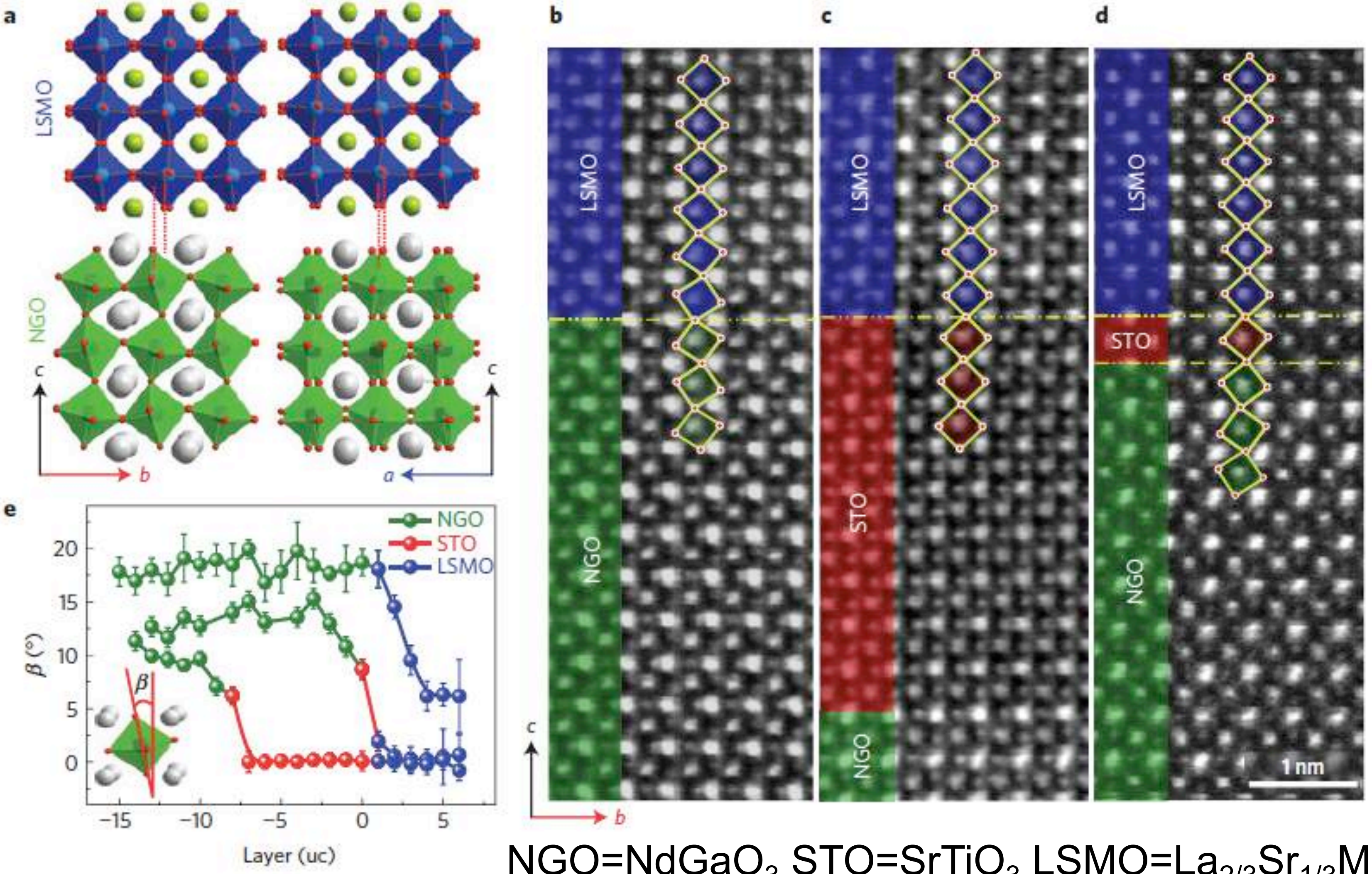

NGO=$NdGaO_3$ STO=$SrTiO_3$ LSMO=$La_{2/3}Sr_{1/3}MnO_3$

Figure 1 | Oxygen octahedral coupling at interfaces in manganite heterostructures. a, Schematic models of atomic ordering in LSMO and NGO crystal structures. **b–d**, Inversed annular bright-field STEM images of LSMO/NGO (**b**), LSMO/STO (9 uc)/NGO (**c**) and LSMO/STO (1 uc)/NGO (**d**) heterostructures. The oxygen atoms are clearly visible, and the connectivity of oxygen octahedra across the interfaces is indicated. All the LSMO films are 6 uc thick. **e**, Layer-position-dependent mean octahedral tilt angle (β) together with its standard deviation in LSMO/NGO heterostructures with and without a STO buffer layer. The data for the non-buffered sample are shifted upwards by 6° for clarity.

Local geometry modified from the bulk for a few u.c.

Liao et al. Nature Mat. 15 (2016) 425

I. Controlling a functionality
(already existing or not in the bulk)

STRAIN-CONTROL in Thin-Films and Heterostructures

→ See lectures 3-4-5 (Nickelates, Ruthenates)
and seminar by Darrell Schlom, May 23
(e.g. Ruthenates)
See also seminar last year June 10, 2016 by Charles Ahn

Sensitivity to pressure in bulk → Strain in thin-films/ Heterostructures

e.g. Nickelates:

RAPID COMMUNICATIONS

PHYSICAL REVIEW B VOLUME 47, NUMBER 18 1 MAY 1993-II

Extraordinary pressure dependence of the metal-to-insulator transition in the charge-transfer compounds $NdNiO_3$ and $PrNiO_3$

P. C. Canfield and J. D. Thompson
Los Alamos National Laboratory, Los Alamos, New Mexico 87545

S-W. Cheong and L. W. Rupp
AT&T Bell Laboratories, Murray Hill, New Jersey 07974

(Received 4 September 1992)

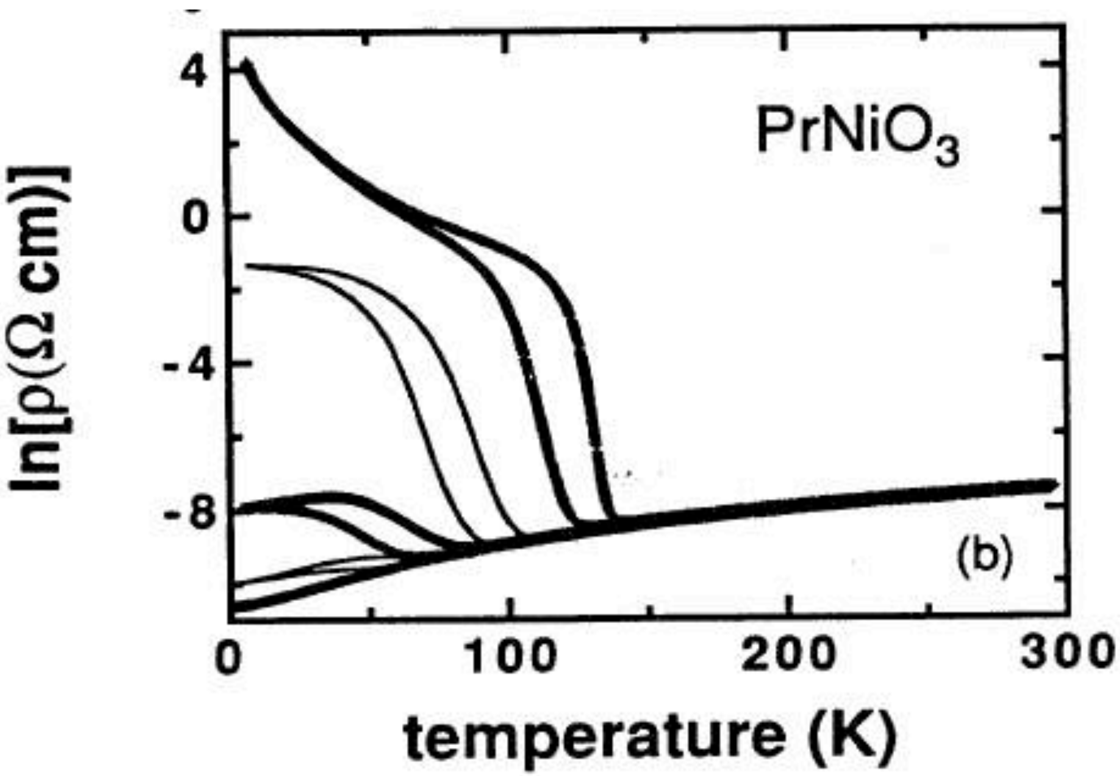

Canfield et al.
PRB 1993

FIG. 2. (a) Temperature-dependent resistivity of $PrNiO_3$ for applied pressures of 1 bar, 5.2 kbar, 9.0 kbar, 10.8 kbar, and 14.1 kbar. Data sets for each pressure are shown alternately as solid lines and crosses. The furthest right data set (crosses) is 1 bar data and the furthest left data set (crosses) is 14.1 kbar data. For each data set the further right curve is the warming data. (Note: for the 14.1 kbar data set there is no hysteresis and therefore no difference between warming and cooling data.) (b) Temperature dependence of the natural log of the resistivity of $PrNiO_3$ at the same pressures.

Strain-Control by growth on different substrates: $RNiO_3$

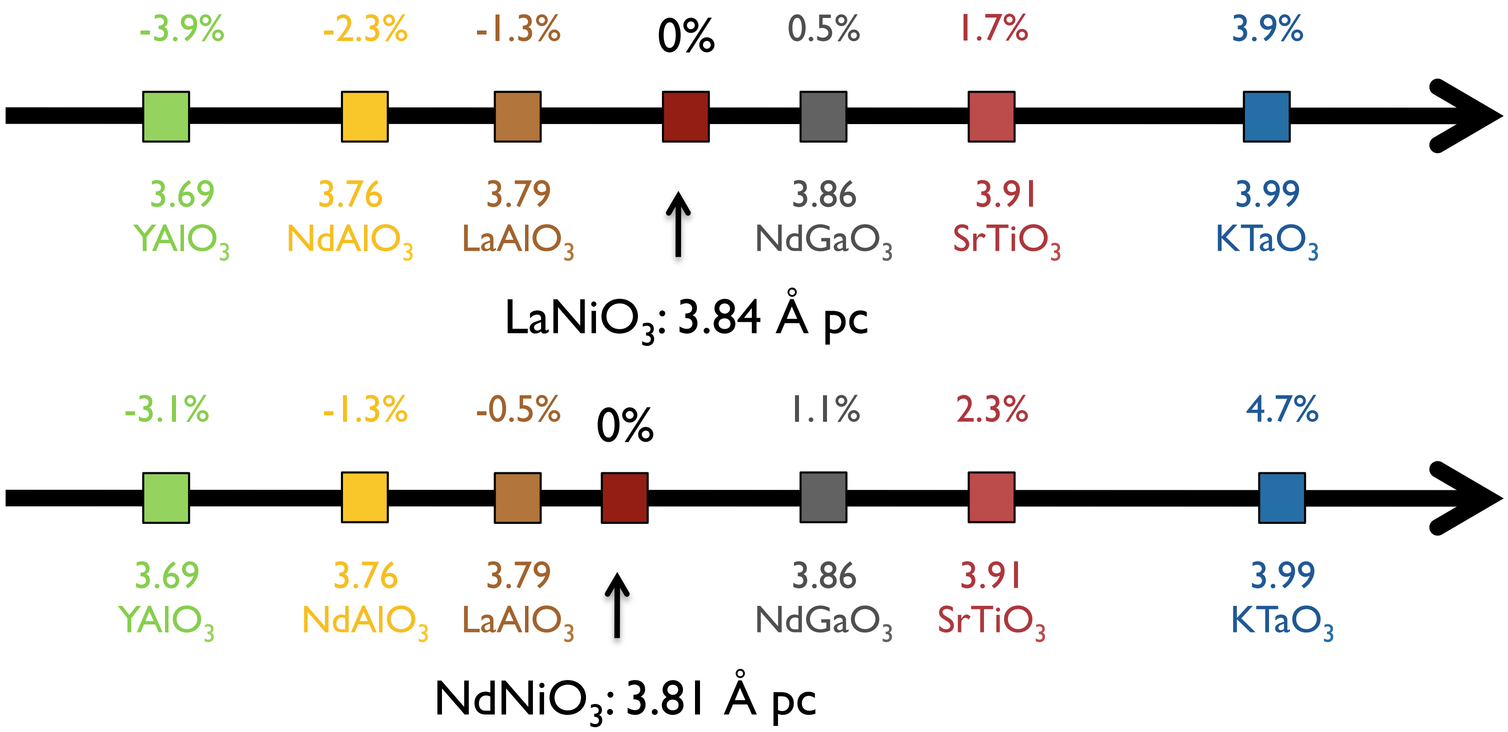

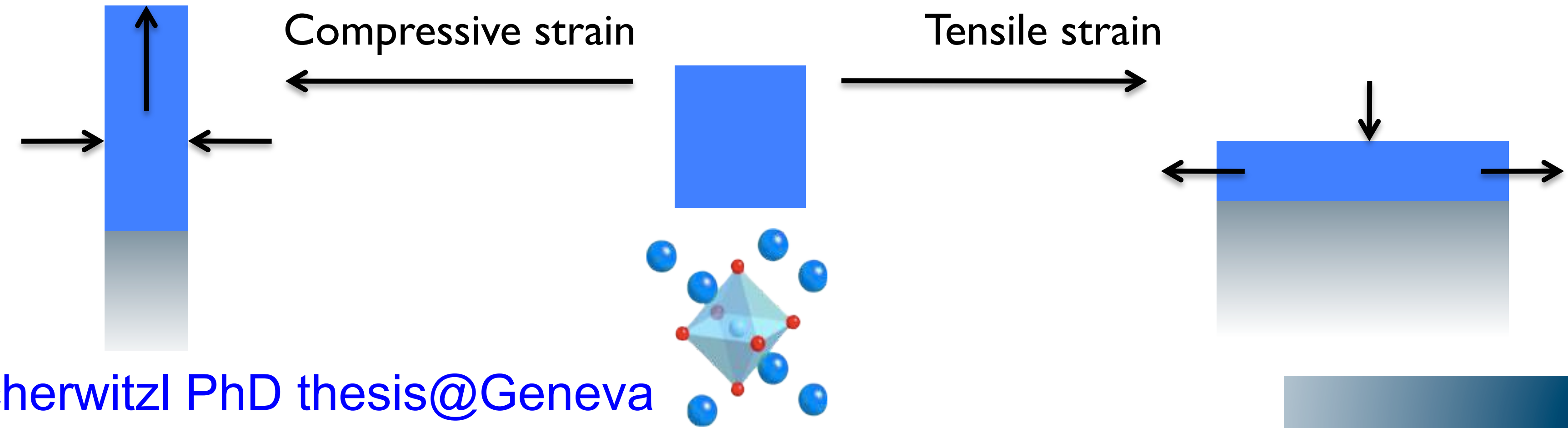

R.Scherwitzl PhD thesis@Geneva

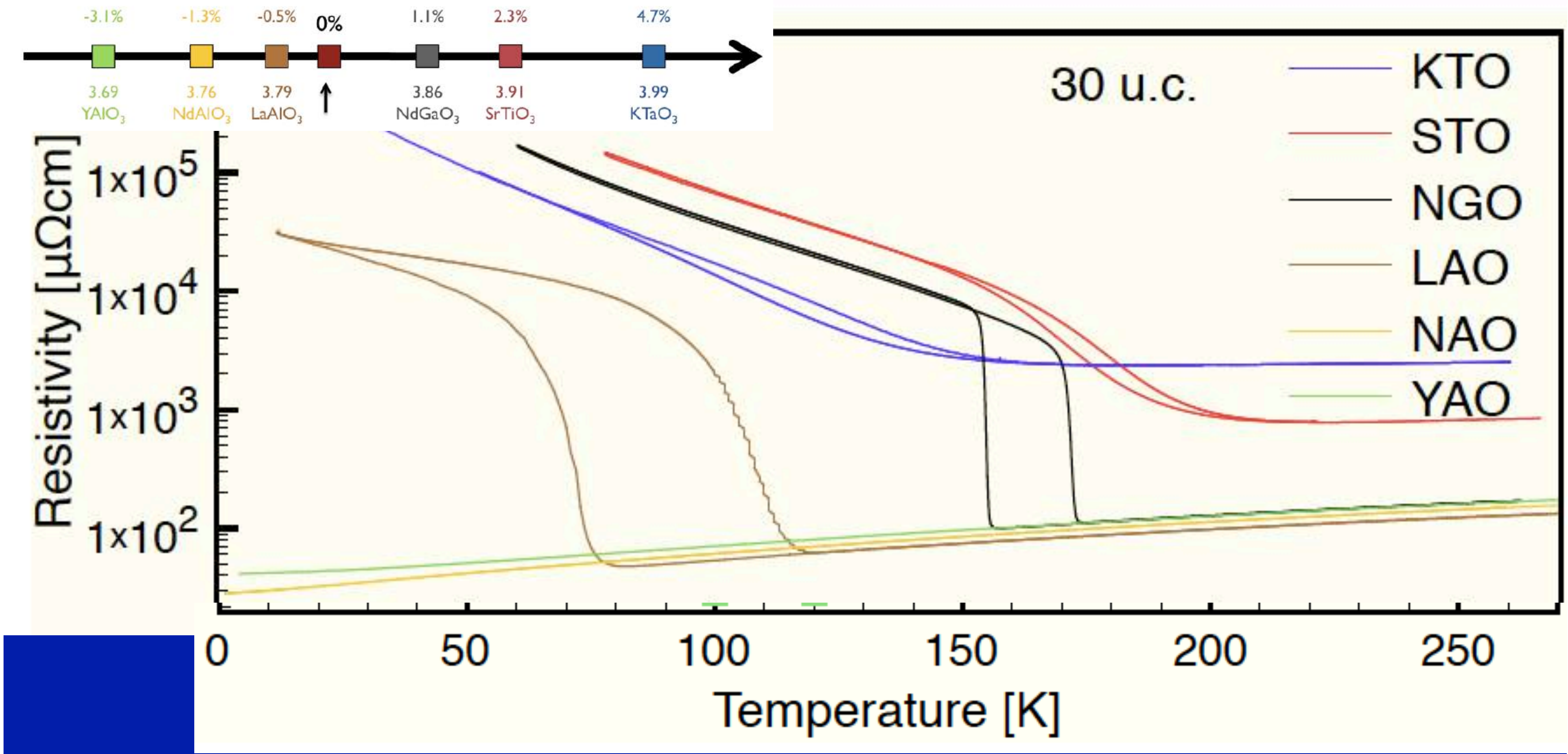

Compressive strain:

- Does not change much resistivity in metallic state (~ 50%)
- Efficiently shifts MIT to lower T, even complete suppression: → NNO ~ LAO

Tensile strain:

- Increases resist in metallic phae
- Smaller shift of MIT to higher T (except KTO: disorder ?)

R.Scherwitzl PhD thesis@Geneva

Multiferroicity induced by tensile strain in $EuTiO_3$

(Lee et al, Nature 466, (2010) 454)

→ D.Schlom seminar May 23 ?

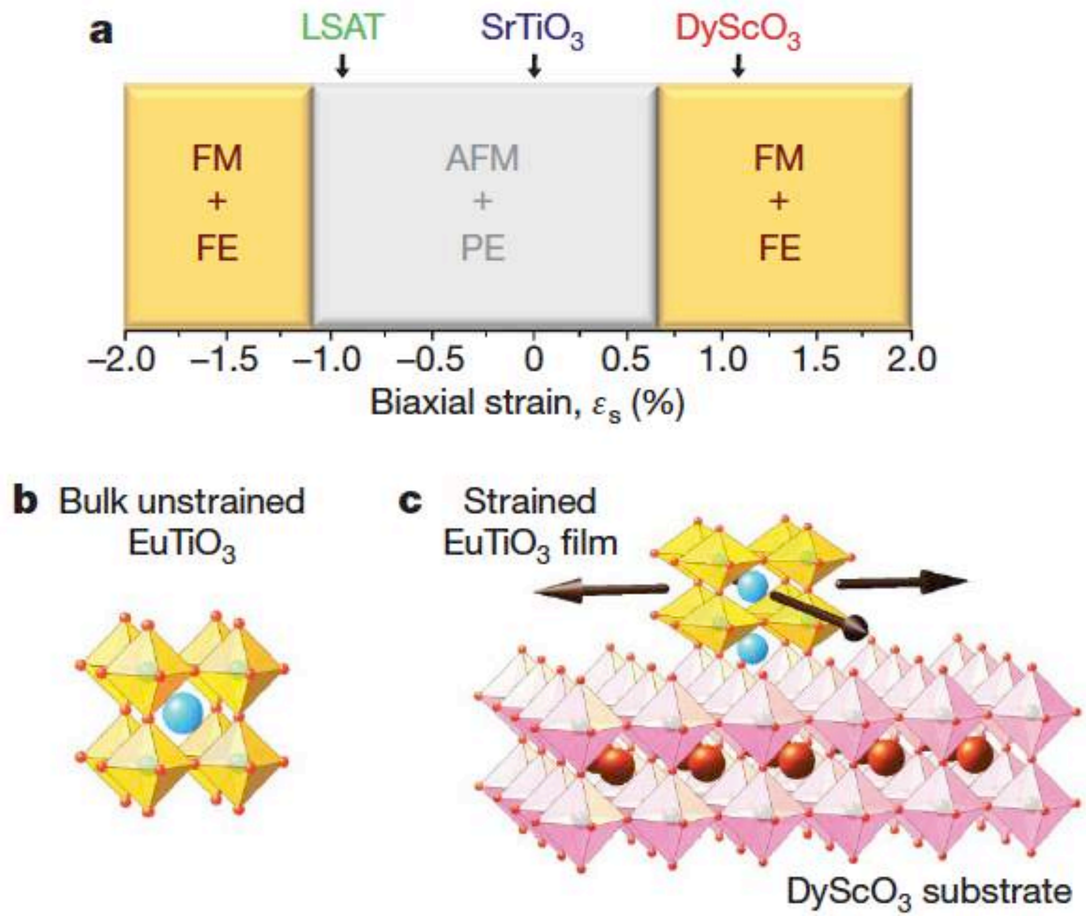

Figure 1 | Predicted effect of biaxial strain on $EuTiO_3$ and our approach to imparting such strain in $EuTiO_3$ films using epitaxy. **a**, First-principles epitaxial phase diagram of $EuTiO_3$ strained from −2% (biaxial compression) to +2% (biaxial tension), calculated in 0.1% steps. Regions with paraelectric (PE), ferroelectric (FE), antiferromagnetic (AFM) and ferromagnetic (FM) behaviour are shown. **b**, **c**, Schematic of unstrained bulk $EuTiO_3$ (**b**) and epitaxially strained thin-film $EuTiO_3$ on the $DyScO_3$ substrate (**c**), showing the in-plane expansion due to biaxial tension.

Control of carrier density by gating, electric field, <u>ionic liquids</u>

→ Seminars by Marcelo Rozenberg May,9 and Manuel Bibes, May 30

Basic principle of a FET

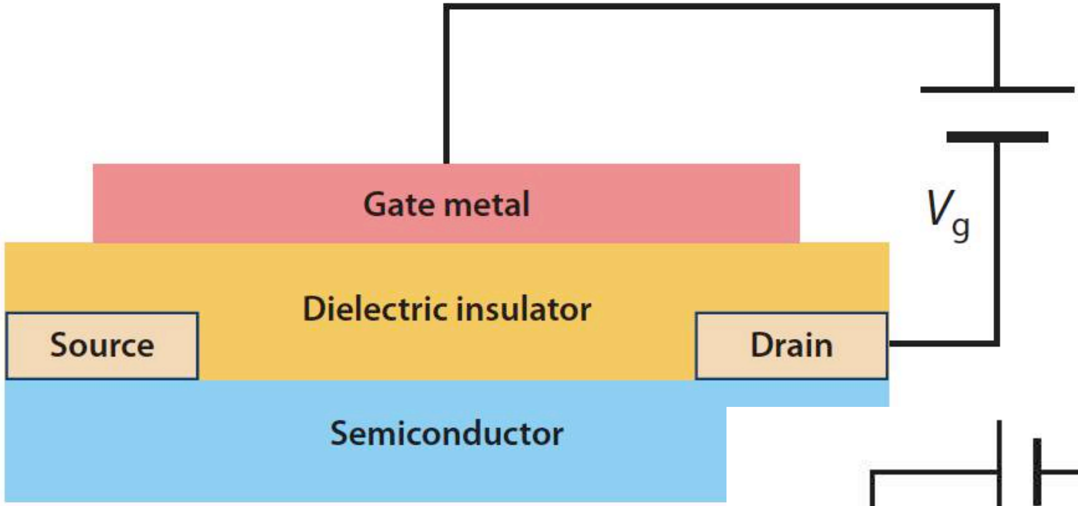

Ionic Liquids

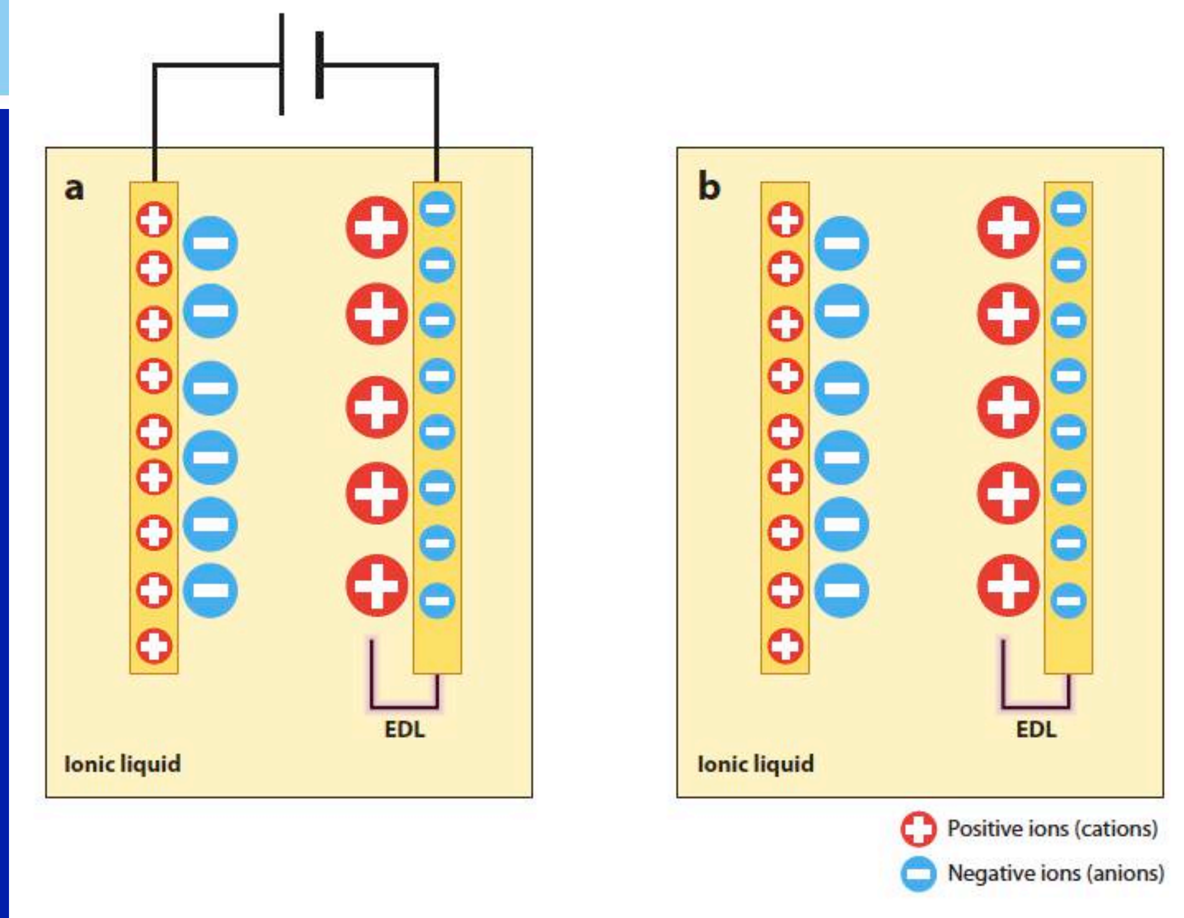

See for reviews:

- A.M.Goldman Annu Rev Mat Res 44:45-63 (2014)
- C.Ahn Rev Mod Phys 78, 1185 (2006)

From conventional FETs to ionic liquids

- K. Ueno *et al.*, *Nature Materials*, (2008)
- J.T. Ye *et al.*, *Nature Materials*, (2009)
- Y. Yamada *et al.*, *Science*, (2011)
- K. Ueno *et al.*, *Nat. Nano.*, (2011)

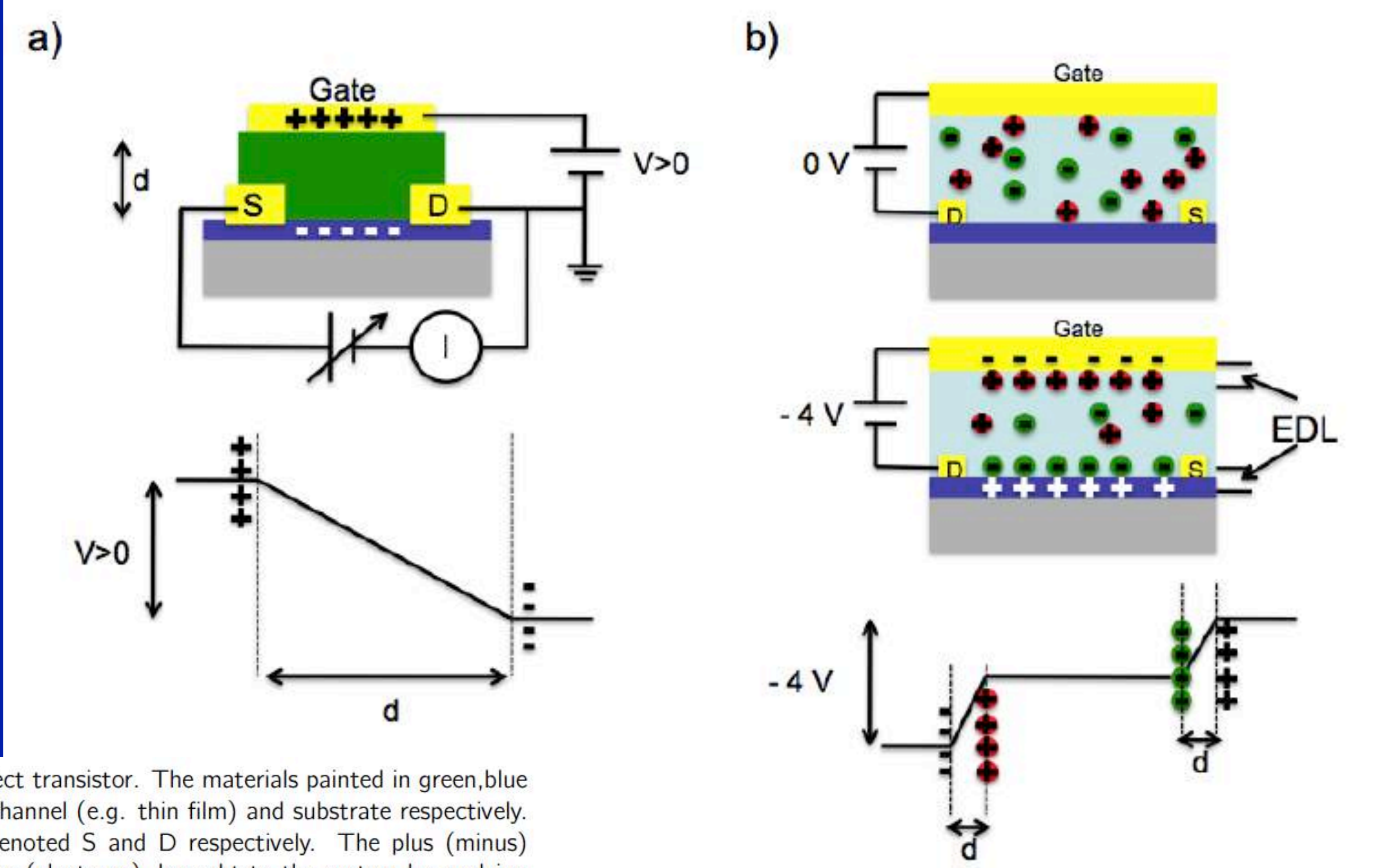

Fig. 4.4: a) Conventional top-gate field-effect transistor. The materials painted in green, blue and grey correspond to the dielectric, the channel (e.g. thin film) and substrate respectively. Source and drain contacts in yellow are denoted S and D respectively. The plus (minus) signs corresponds to electrical charges, holes (electrons), brought to the system by applying a voltage V to the gate. A voltage is applied at the same time between the source and the grounded drain contact and the current is measured. Below, a sketch of the voltage drop across the dielectric across its thickness d. b) Liquid-gate field-effect transistor with 0 V and -4 V applied. The red and green charges represent cations and anions respectively. With applied gate voltage two electric double layers (EDL) form. The voltage drop across the liquid is sketched below.

Carrier densities of 10^{14}-10^{15} cm^{-2} can be achieved ! (~ 3 orders of mag. larger than with SiO_2 gating)

Field-control of MIT in $NdNiO_3$ on $LaAlO_3$

R.Scherwitzl et al.
Adv. Mat. 22, 5517 (2010)

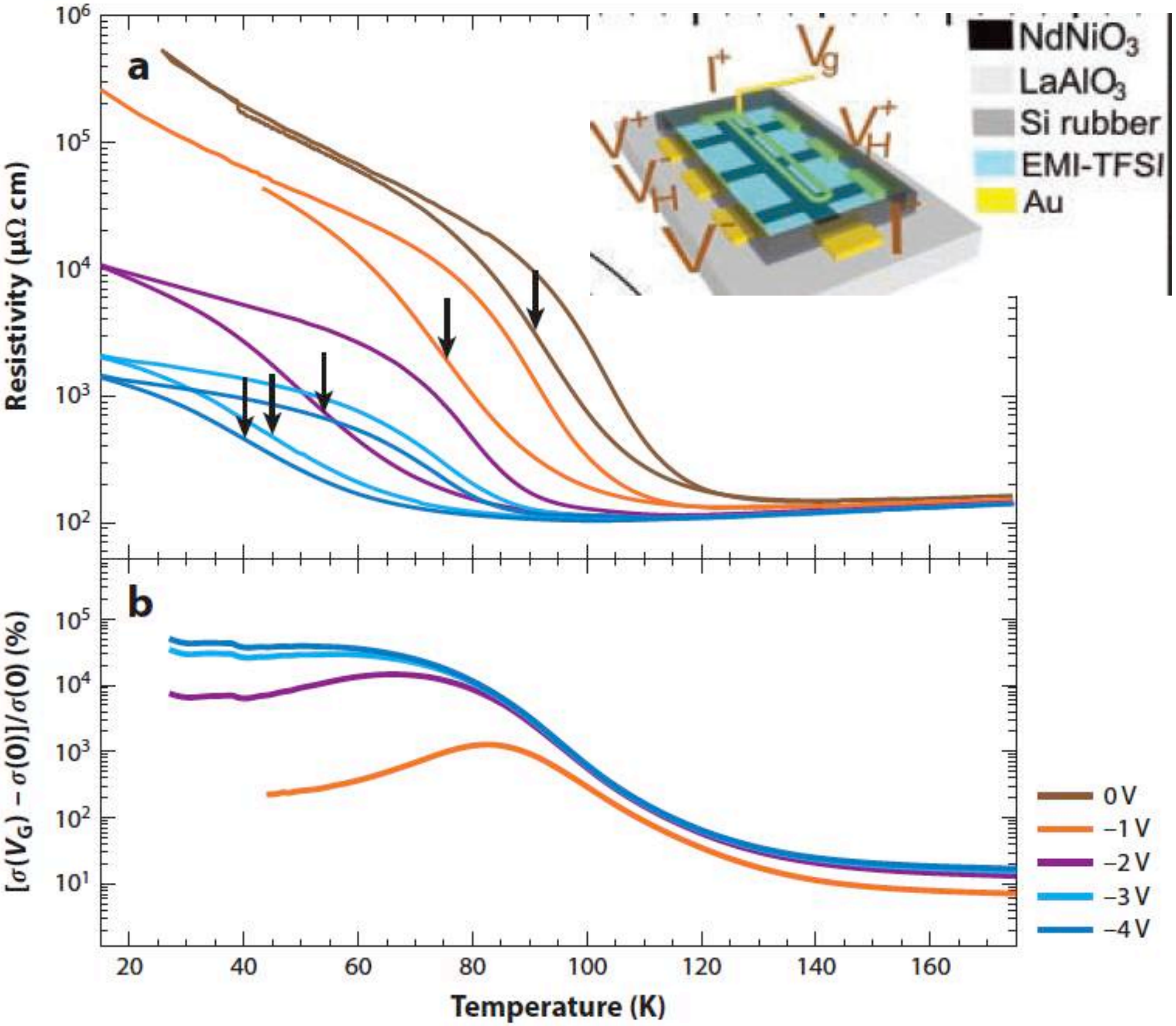

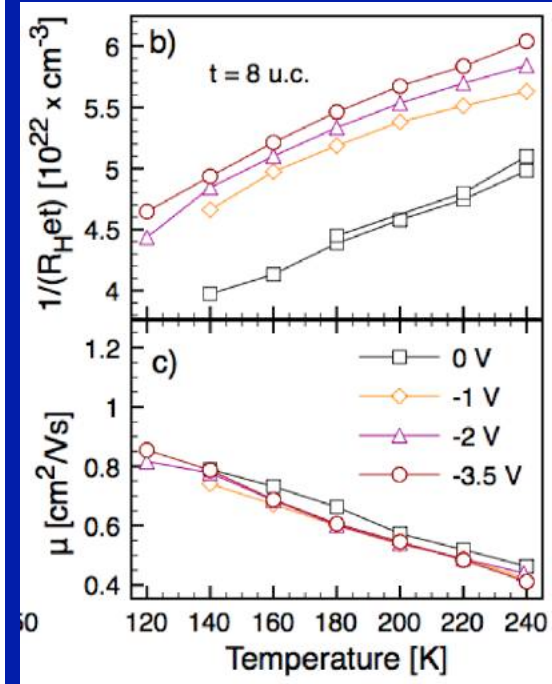

Electric field control of a metal-insulator transition. (*a*) Modulation of the metal-insulator transition temperature in ultrathin films of $NdNiO_3$ by using an ionic liquid gate. Arrows represent the nominal transition temperature of the metal-insulator transition. (*b*) Electroconductivity as a function of temperature and applied gate voltage. Reproduced with permission from Reference 26.

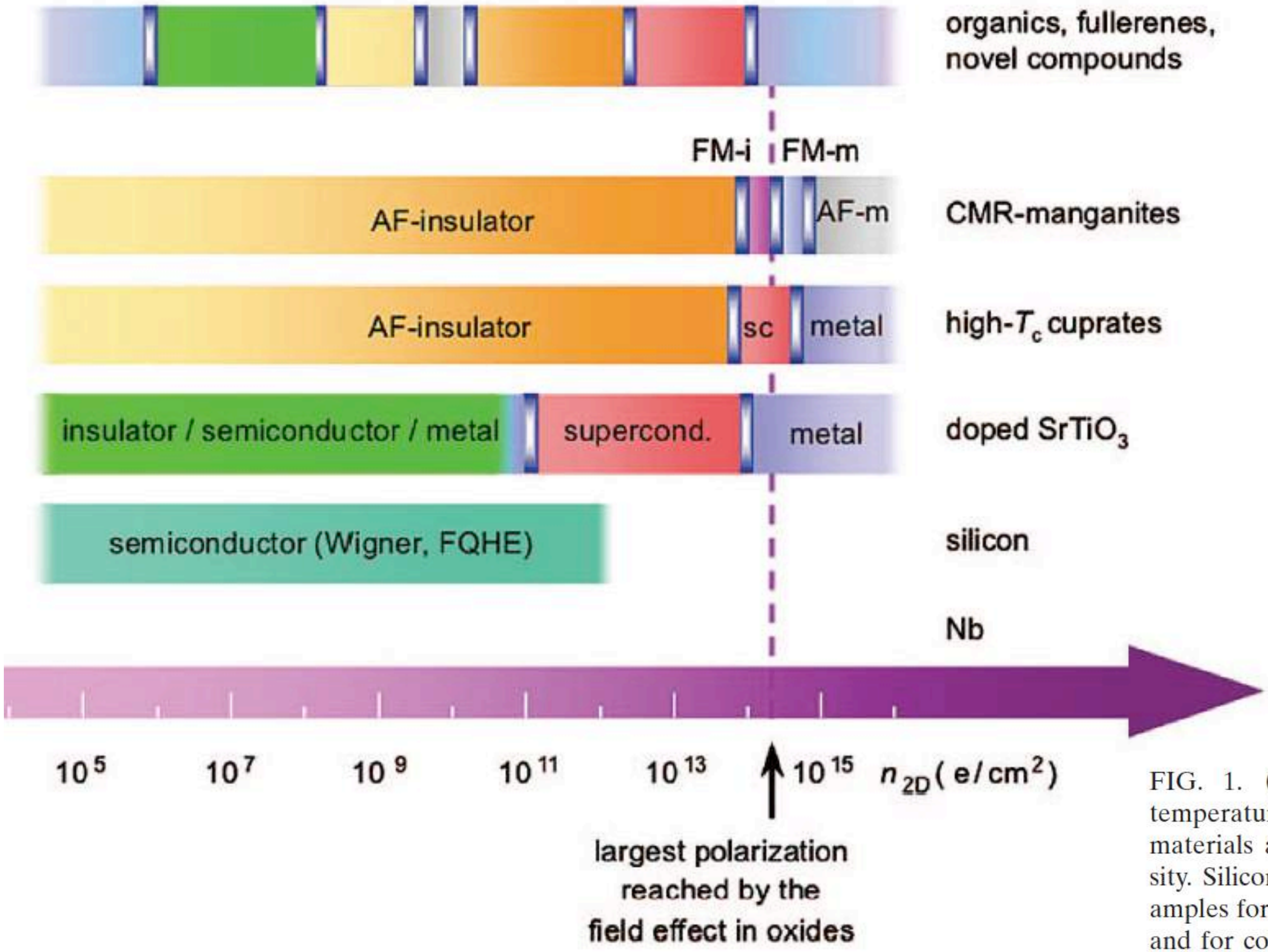

FIG. 1. (Color) Illustration of the zero-temperature behavior of various correlated materials as a function of sheet charge density. Silicon is shown as a reference. The examples for high-temperature superconductors and for colossal magnetoresistive manganites reflect $YBa_2Cu_3O_7$ and $(La,Sr)MnO_3$, respectively. Top bar shows schematically the richness of materials available for field-effect tuning and the spectrum of their phases. AF, FM, I, M, SC, FQHE, and Wigner stand for antiferromagnetic, ferromagnetic, insulator, metal, superconductor, fractional quantum Hall effect, and Wigner crystal, respectively. From Ahn *et al.*, 2003.

Ahn, Triscone and Mannhart
Nature 424, 1015 (2003)
Ahn et al. Rev Mod Phys 78, 1185 (2006)

Turning an insulator into a Super-conductor by gating

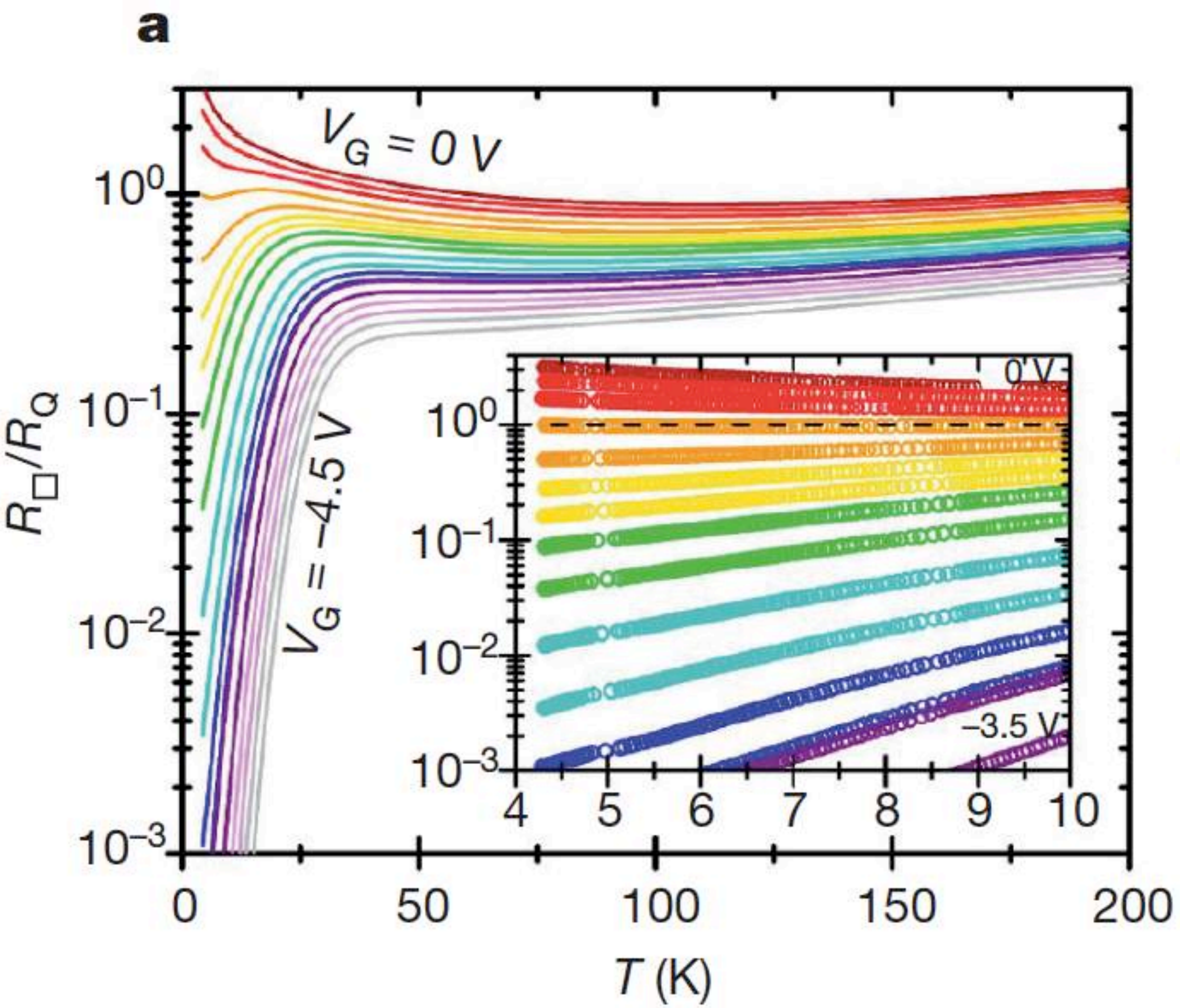

LETTER

doi:10.1038/nature09998

Nature 472, 458 (2011)

Superconductor–insulator transition in $La_{2-x}Sr_xCuO_4$ at the pair quantum resistance

A. T. Bollinger[1], G. Dubuis[1,2], J. Yoon[1], D. Pavuna[2], J. Misewich[1] & I. Božović[1]

Inducing SC by ionic-liquid gating !

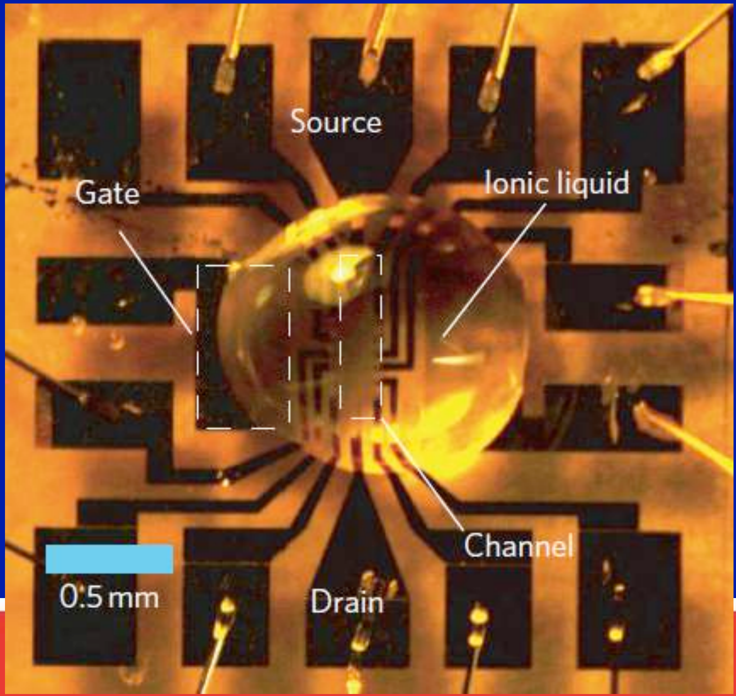

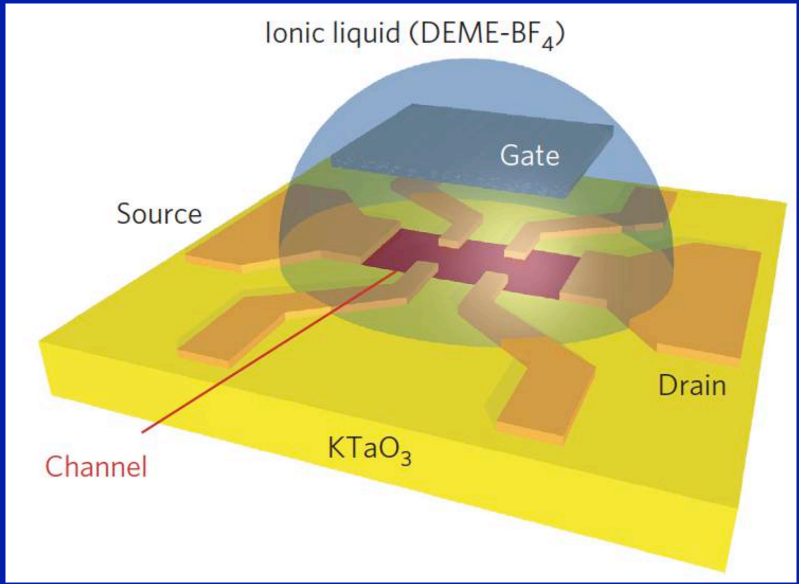

LETTERS
PUBLISHED ONLINE: 22 MAY 2011 | DOI: 10.1038/NNANO.2011.78
nature nanotechnology

Discovery of superconductivity in $KTaO_3$ by electrostatic carrier doping

K. Ueno[1,2], S. Nakamura[3,4], H. Shimotani[5], H. T. Yuan[5], N. Kimura[4,6], T. Nojima[3,4], H. Aoki[4,6], Y. Iwasa[5,7] and M. Kawasaki[1,5,7]*

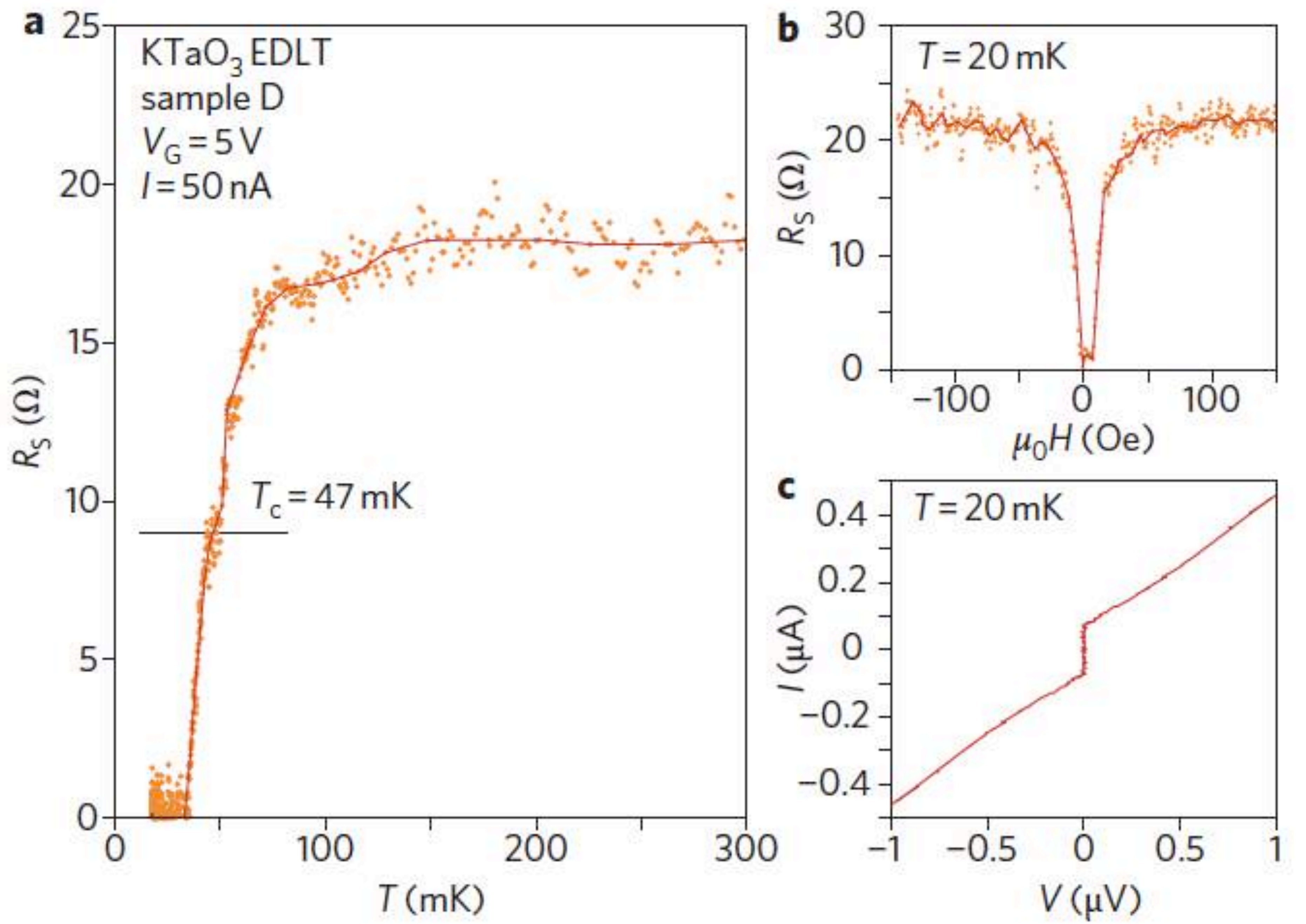

a
KTaO3 EDLT
sample D
VG = 5 V
I = 50 nA
Tc = 47 mK
RS (Ω)
T (mK)
0
100
200
300
0
5
10
15
20
25
b
T = 20 mK
RS (Ω)
μ0H (Oe)
−100
0
100
0
10
20
30
c
T = 20 mK
I (μA)
V (μV)
−1
−0.5
0
0.5
1
−0.4
−0.2
0
0.2
0.4

Superconductivity at 100K in monolayer FeSe !

CHIN. PHYS. LETT. Vol. 29, No. 3 (2012) 037402

Interface-Induced High-Temperature Superconductivity in Single Unit-Cell FeSe Films on $SrTiO_3$ *

WANG Qing-Yan(王庆艳)[1,2†], LI Zhi(李志)[2†], ZHANG Wen-Hao(张文号)[1†], ZHANG Zuo-Cheng(张祚成)[1†], ZHANG Jin-Song(张金松)[1], LI Wei(李渭)[1], DING Hao(丁浩)[1], OU Yun-Bo(欧云波)[2], DENG Peng(邓鹏)[1], CHANG Kai(常凯)[1], WEN Jing(文竞)[1], SONG Can-Li(宋灿立)[1], HE Ke(何珂)[2], JIA Jin-Feng(贾金锋)[1], JI Shuai-Hua(季帅华)[1], WANG Ya-Yu(王亚愚)[1], WANG Li-Li(王立莉)[2], CHEN Xi(陈曦)[1], MA Xu-Cun(马旭村)[2**], XUE Qi-Kun(薛其坤)[1**]

[1] *State Key Lab of Low-Dimensional Quantum Physics, Department of Physics, Tsinghua University, Beijing 100084*
[2] *Institute of Physics, Chinese Academy of Sciences, Beijing 100190*

nature materials

LETTERS

PUBLISHED ONLINE: 24 NOVEMBER 2014 | DOI: 10.1038/NMAT4153

Superconductivity above 100 K in single-layer FeSe films on doped $SrTiO_3$

Jian-Feng Ge[1], Zhi-Long Liu[1], Canhua Liu[1,2*], Chun-Lei Gao[1,2], Dong Qian[1,2], Qi-Kun Xue[3*], Ying Liu[1,2,4] and Jin-Feng Jia[1,2*]

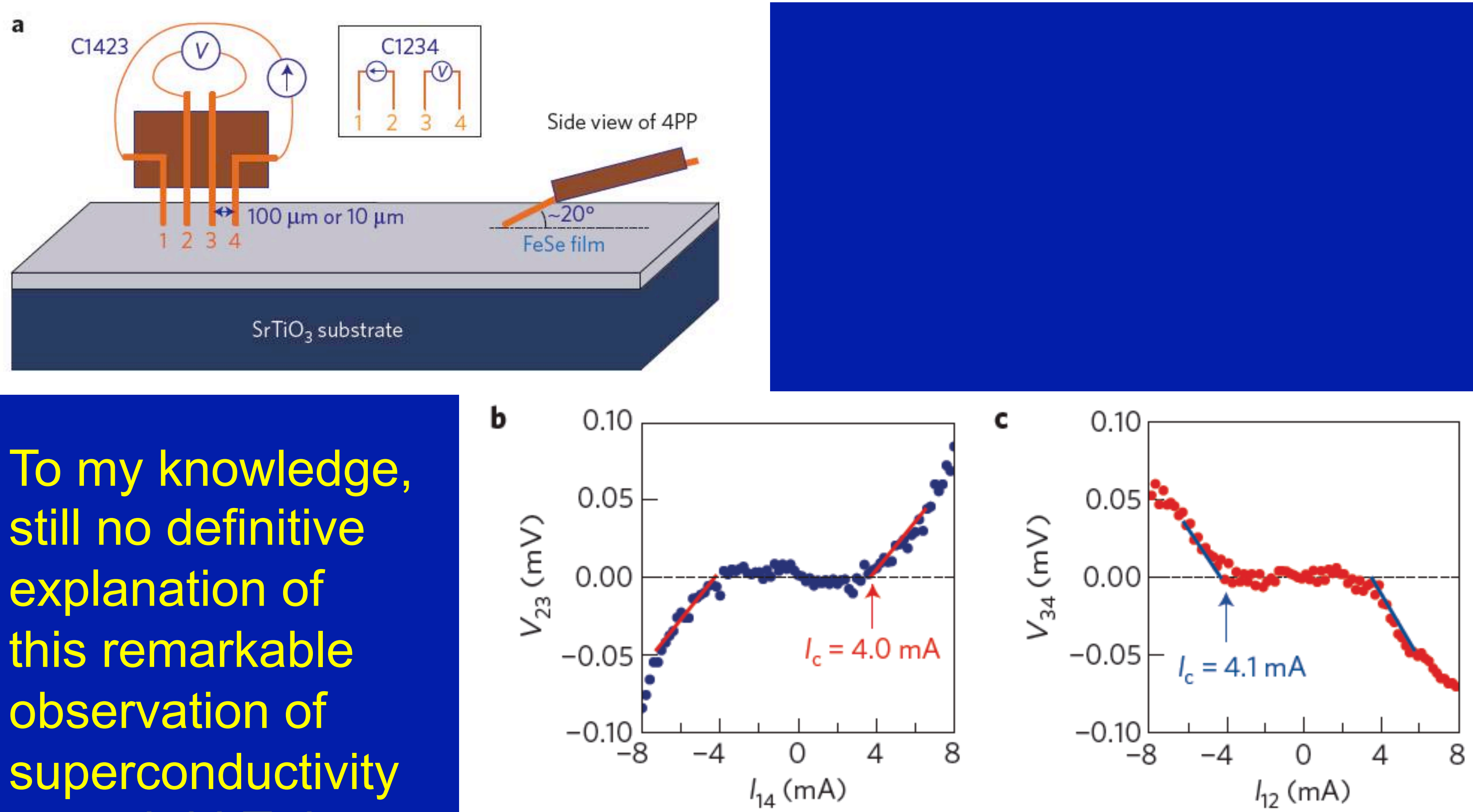

Figure 2 | 4PP transport measurement set-up. a, Schematic of the 4PP transport measurement set-up. The numbers are used to denote the contacting tips. All four tips can touch the sample surface gently at an inclined angle of ~20°. The inset shows schematically the measurement configuration C1234. **b**,**c**, Typical superconducting *I*–*V* curves taken with a tip separation of 10 μm at 3.0 K with measurement configurations C1423 and C1234, respectively.

To my knowledge, still no definitive explanation of this remarkable observation of superconductivity at such hi-T_c in monolayer FeSe !

II. Engineering a new functionality by combining two (or more) materials

letters to nature

Nature 419, 378 (2002)

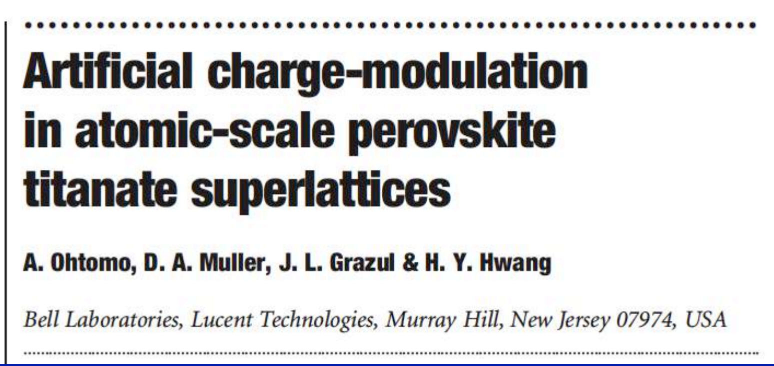

Artificial charge-modulation in atomic-scale perovskite titanate superlattices

A. Ohtomo, D. A. Muller, J. L. Grazul & H. Y. Hwang

Bell Laboratories, Lucent Technologies, Murray Hill, New Jersey 07974, USA

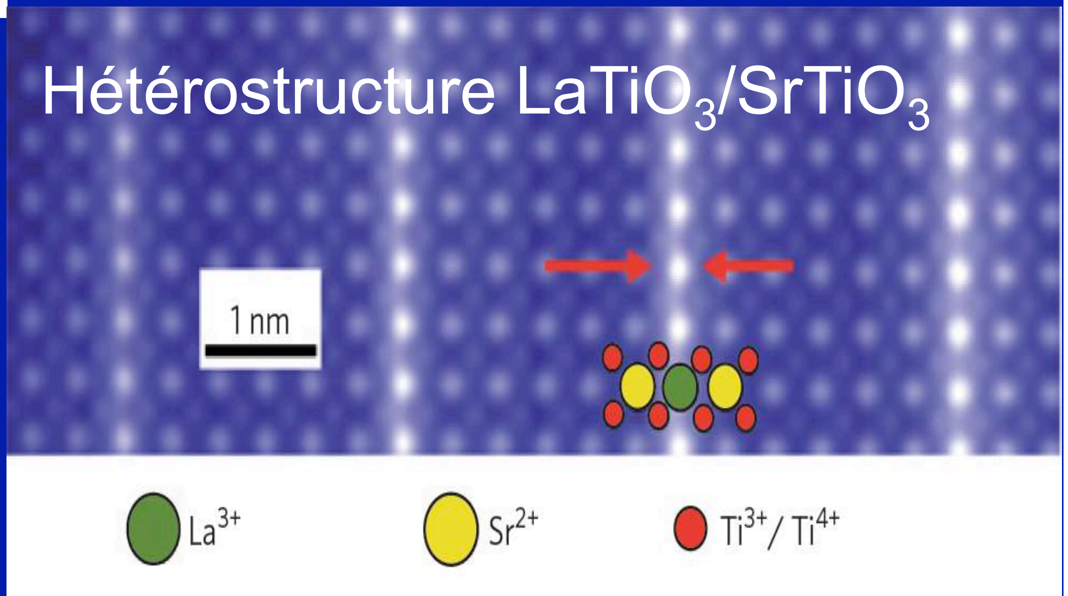

Creating a Metal out of two Insulators…

$LaTiO_3$ Mott insulator Ti^{3+} $3d^1$

/ $SrTiO_3$ band insulator Ti^{4+} $3d^0$

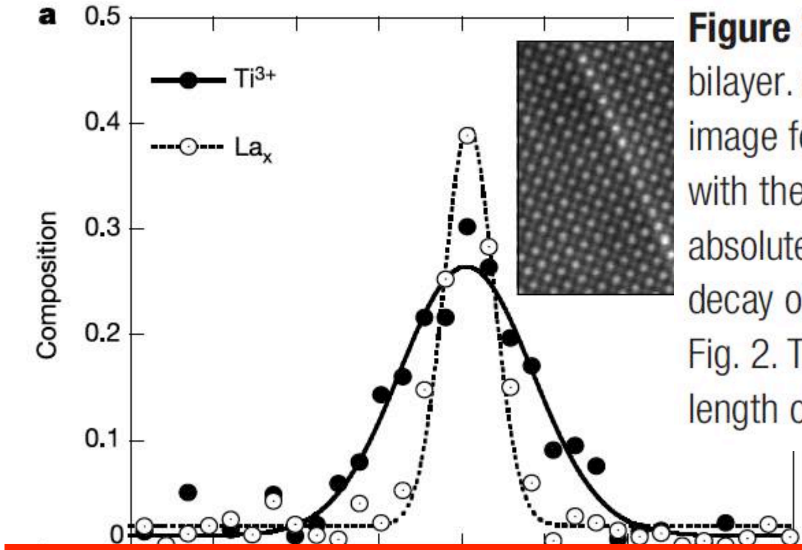

Figure 3 Spatial distribution of the Ti^{3+} signal in the vicinity of the $LaTiO_3$ layer and bilayer. **a**, EELS profiles for La and Ti recorded across a $LaTiO_3$ monolayer. Inset, the ADF image for the monolayer (layer '1' in Fig. 1). The La M edge is recorded simultaneously with the Ti L edge, yet the Ti^{3+} signal is considerably wider than that of the La. The absolute fractions of La and Ti^{3+} were calibrated from bulk $LaTiO_3$ and $SrTiO_3$. **b**, The decay of the Ti^{3+} signal away from the $LaTiO_3$ monolayer of **a** as well as the bilayer of Fig. 2. The tails of the Ti^{3+} signal for both structures fit an exponential decay with a decay length of $\lambda = 1.0 \pm 0.2$ nm.

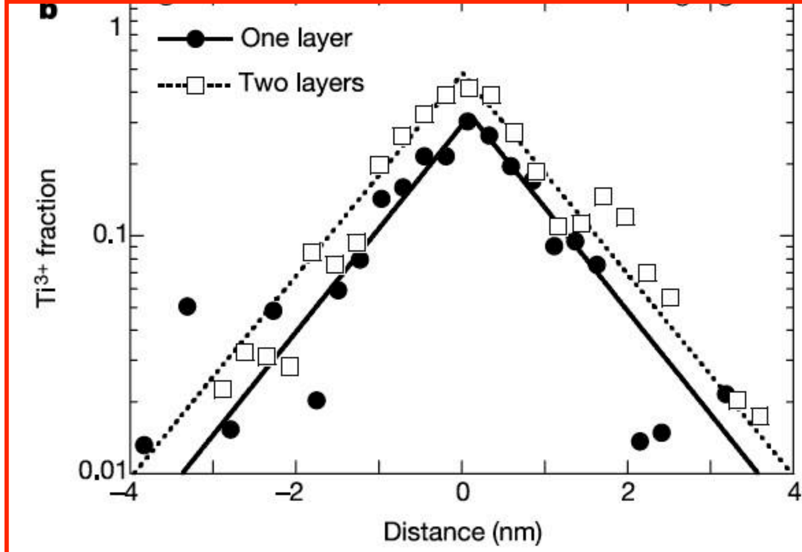

1-layer $(LTO)_1(STO)_{10}$ - EELS
Only ~ 30% of Ti in Ti^{3+} configuration

Very rapid variation over distance from interface: exponential with characteristic length ~ 1nm

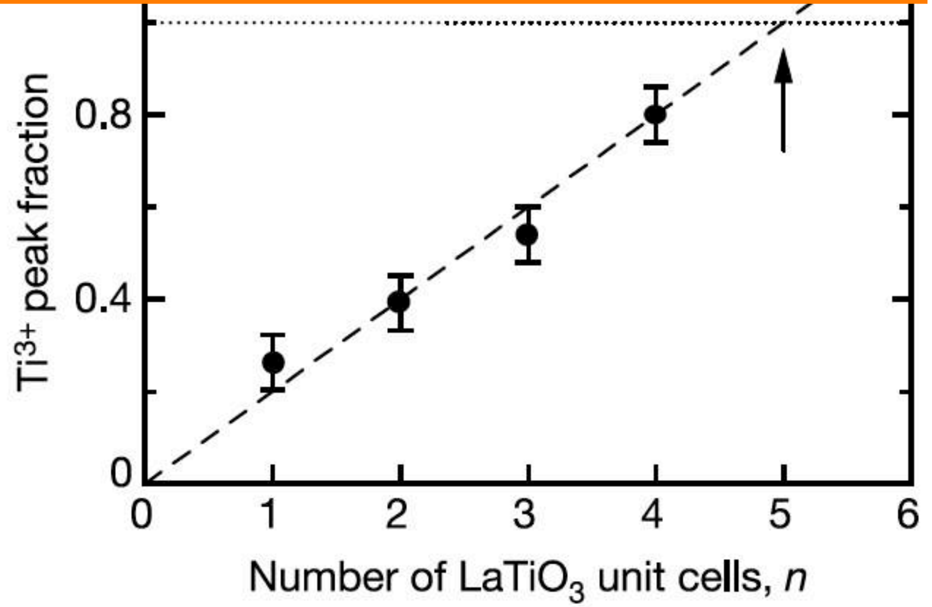

It takes about 5 layers to reach 100% of Ti in Ti^{3+} configuration, as in bulk

$(STO)_m$ $(LTO)_n$ samples are metallic, as is $La_xSr_{1-x}TiO_3$ in bulk

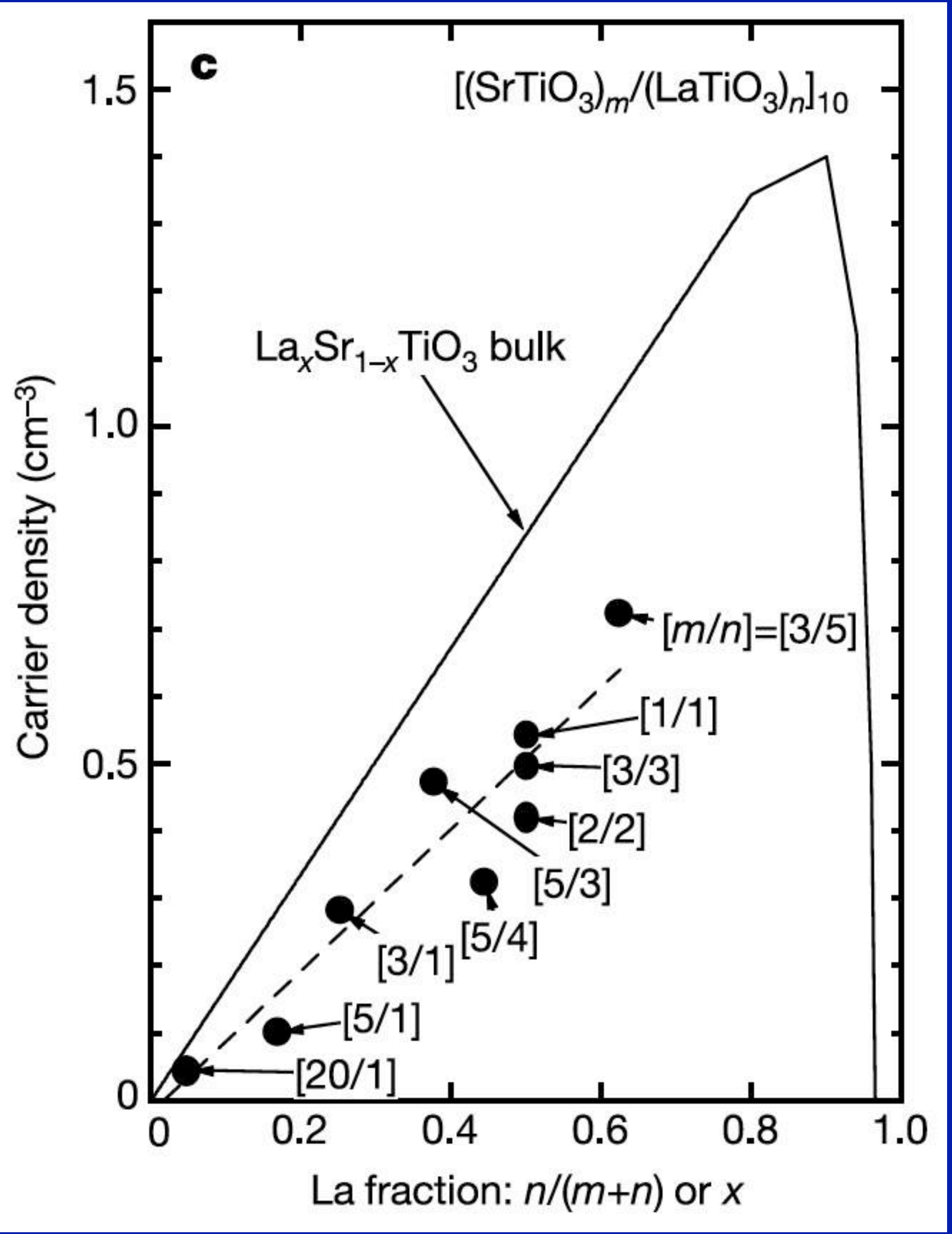

Carrier density from Hall effect

LETTER

doi:10.1038/nature19343

Atomically engineered ferroic layers yield a room-temperature magnetoelectric multiferroic

Julia A. Mundy[1*], Charles M. Brooks[2*], Megan E. Holtz[1*], Jarrett A. Moyer[3], Hena Das[1], Alejandro F. Rébola[1], John T. Heron[2,4], James D. Clarkson[5], Steven M. Disseler[6], Zhiqi Liu[5], Alan Farhan[7], Rainer Held[2], Robert Hovden[1], Elliot Padgett[1], Qingyun Mao[1], Hanjong Paik[2], Rajiv Misra[8], Lena F. Kourkoutis[1,9], Elke Arenholz[7], Andreas Scholl[7], Julie A. Borchers[6], William D. Ratcliff[6], Ramamoorthy Ramesh[5,10,11], Craig J. Fennie[1], Peter Schiffer[3], David A. Muller[1,9] & Darrell G. Schlom[2,9]

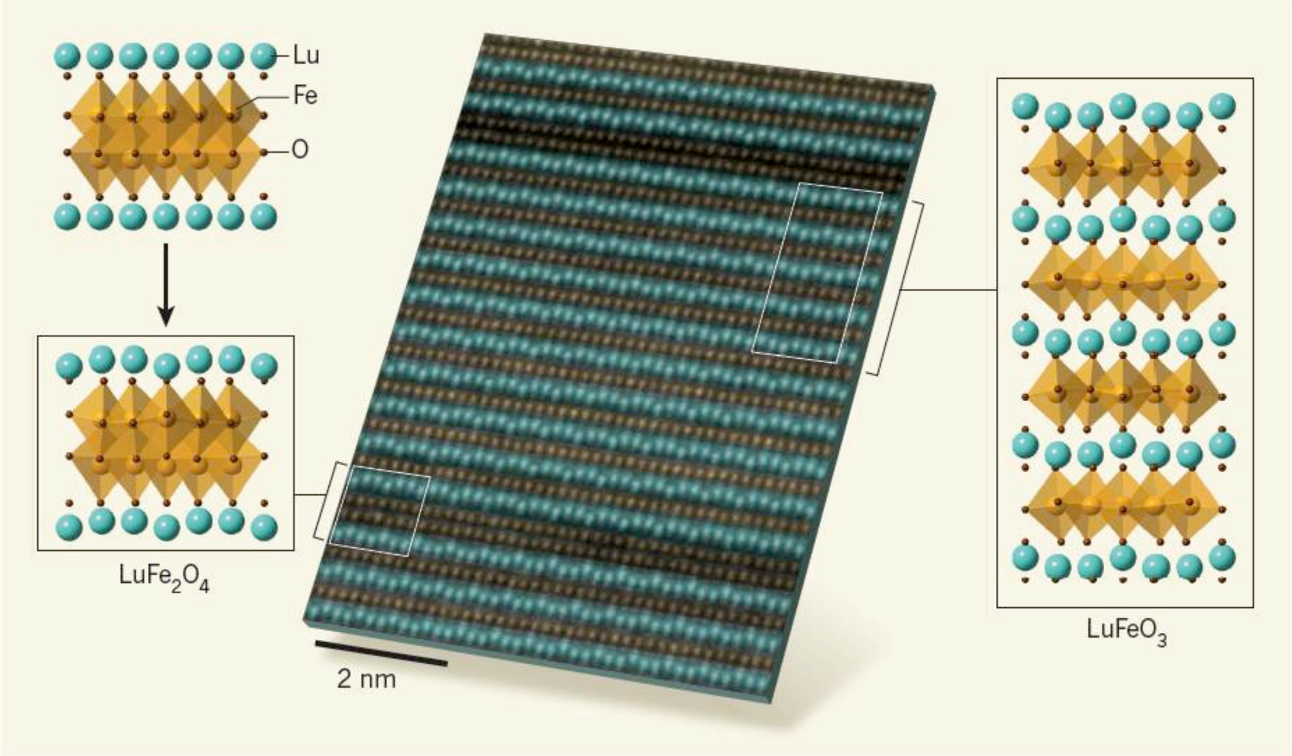

Figure 1 | A new multiferroic material. Mundy *et al.*[2] have constructed a material that exhibits coupled magnetization and electric polarization at higher temperatures than most existing multiferroics. The authors present a scanning transmission electron microscopy (STEM) image of their multiferroic (centre, shown in false colour). The material is a combination of $LuFe_2O_4$ and $LuFeO_3$, whose crystal structures are shown on the left and right sides of the STEM image, respectively. The corrugated structure of $LuFeO_3$ modifies the structure of $LuFe_2O_4$ (indicated by the arrow) and the result is a self-stabilizing multiferroic material.

III. Creating 2D Electron Gases and Electron Liquids at oxide interfaces with interesting properties

`Often, it may be said that

the interface is the device'

H.Kroemer Nobel's lecture

The Polar `Catastrophe' (actually: Polar Blessing !)

Example of a POLAR interface: $LaAlO_3/SrTiO_3$ [LAO/STO]

- Along e.g. the (pseudocubic) 001 direction, an ABO_3 oxide is made of alternating planes of AO and BO_2

- For STO: $Sr^{2+}O^{2-}$ and $Ti^{4+}[O_2]^{4-}$: NEUTRAL

- For LAO: $La^{3+}O^{2-}$ and $Al^{3+}[O_2]^{4-}$:
ALTERNATING 1+/1- CHARGES

Once the two materials are put in contact, an issue arises: what will happen due to this charge mismatch ?

LAO with an (unreconstructed) boundary: DIVERGING V(x) !

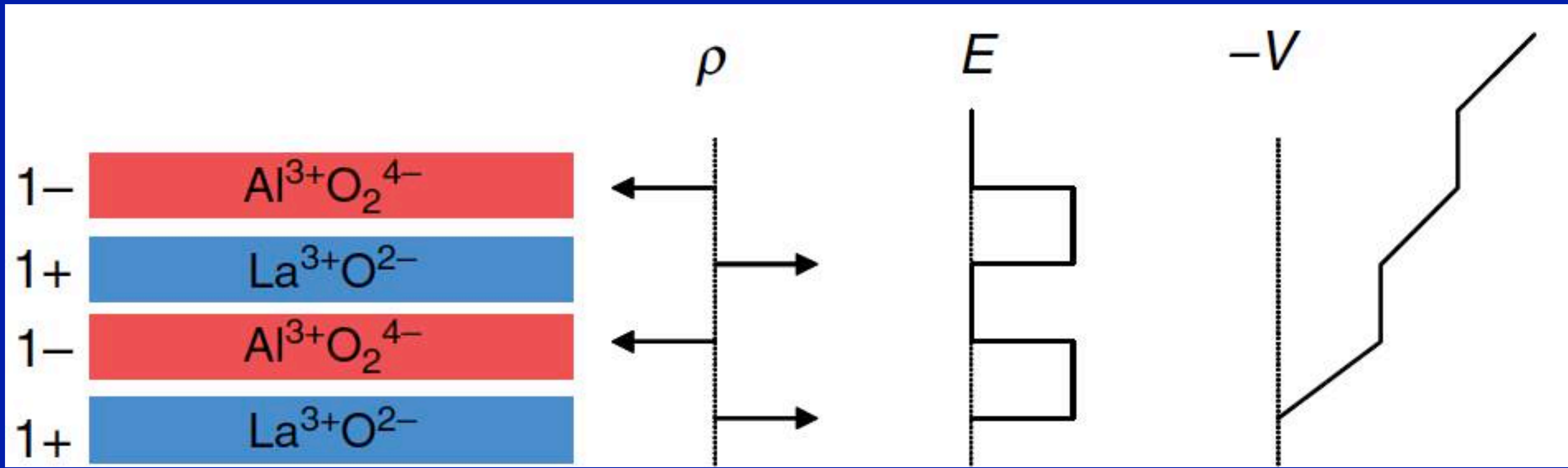

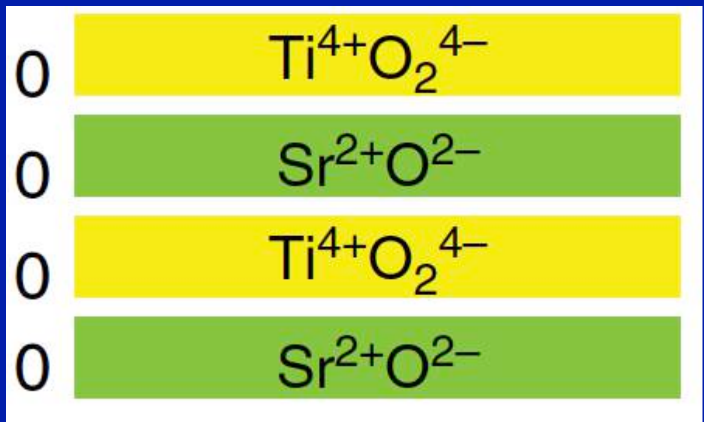

Each LaO layer can be viewed as giving one unit of charge to each AlO_2 layer

Poisson equation (very naïve, in reality: screening, Thomas-Fermi etc.):

$$\frac{\partial E}{\partial x} \equiv -\frac{\partial^2 V}{\partial x^2} = \frac{\rho}{\varepsilon_0} \Rightarrow E(x) = \int^x dx' \, \frac{\rho(x')}{\varepsilon_0}$$

This `polar catastrophe' can be resolved by shifting the charge distribution to create a 2D charged layer at the interface, with ½ e par unit cell:

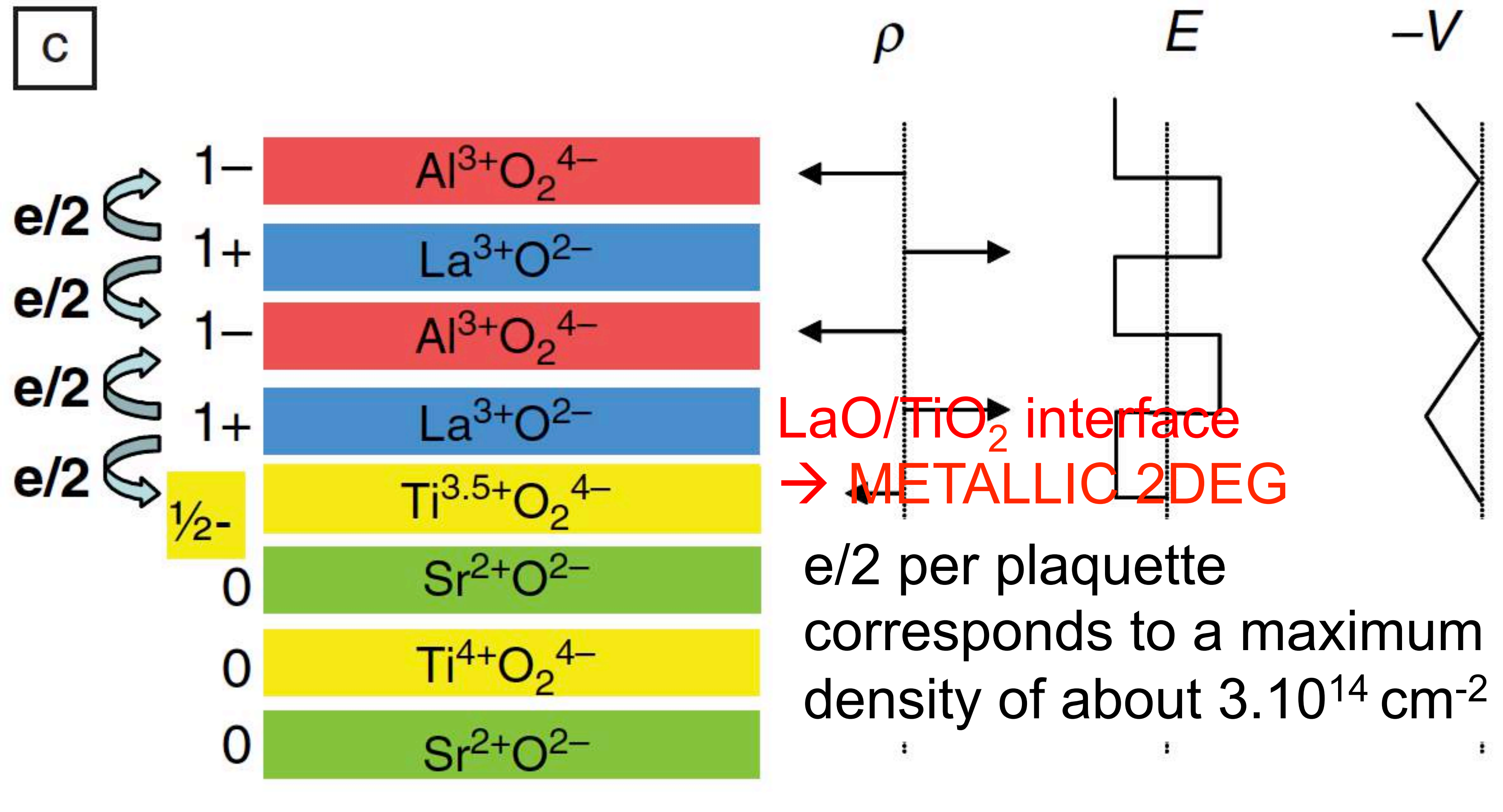

e/2 per plaquette corresponds to a maximum density of about 3.10^{14} cm^{-2}

NB: Something must happen at the top layer, not discussed here (such as structural reconstruction or another 2DEG)

The AlO_2/SrO interface would naively also lead to a 2DEG with this time max ½ hole per unit cell corresponding to oxygen vacancies. However <u>insulating</u> behavior is found (carriers not mobile, reconstruction ?)

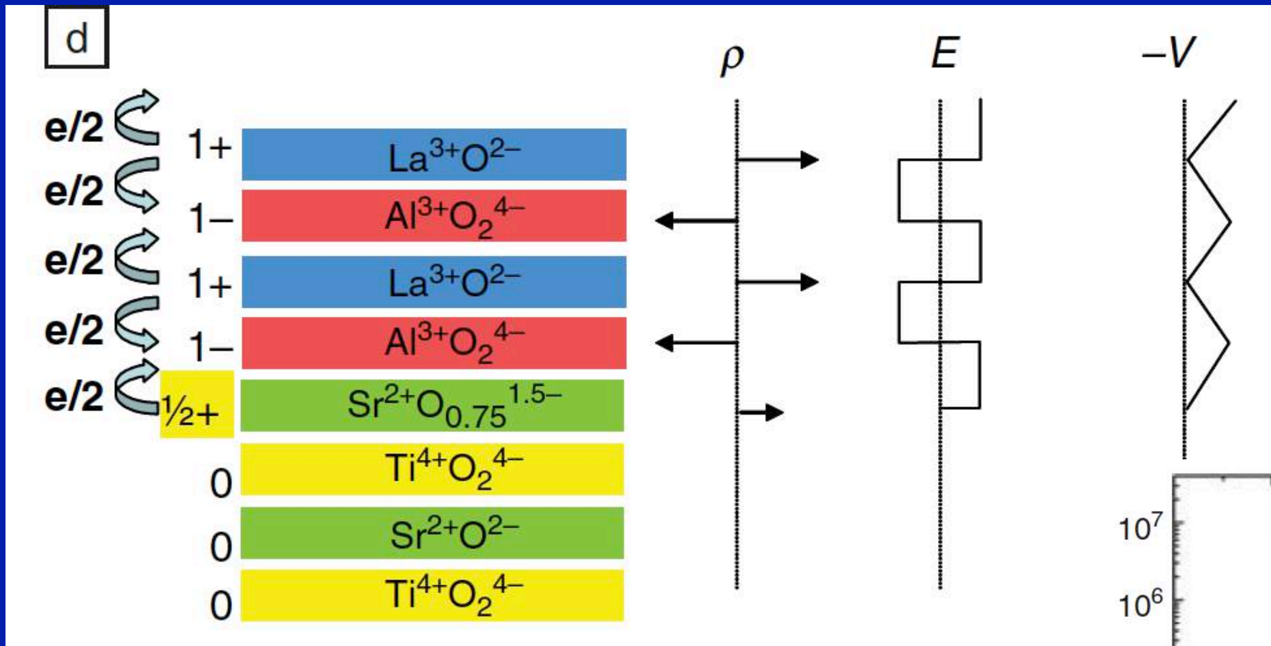

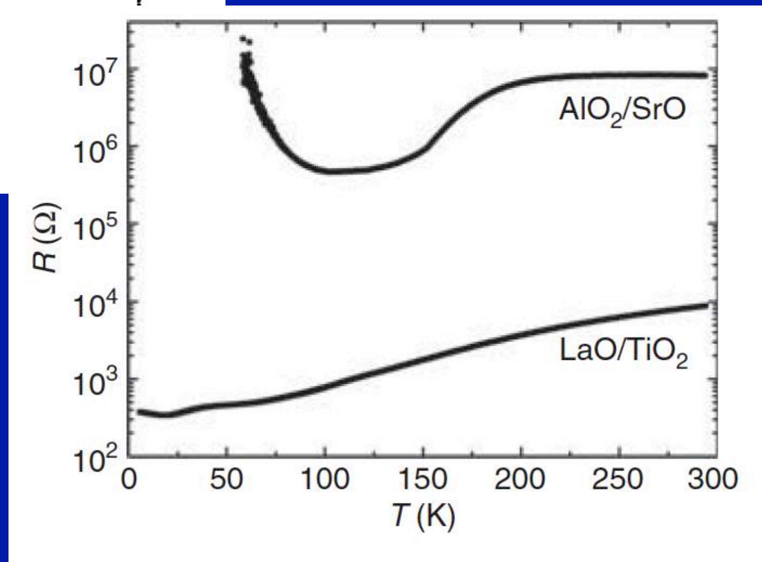

Discovery of Superconductivity at the LAO/STO interface !

Superconducting Interfaces Between Insulating Oxides

N. Reyren,[1] S. Thiel,[2] A. D. Caviglia,[1] L. Fitting Kourkoutis,[3] G. Hammerl,[2] C. Richter,[2] C. W. Schneider,[2] T. Kopp,[2] A.-S. Rüetschi,[1] D. Jaccard,[1] M. Gabay,[4] D. A. Muller,[3] J.-M. Triscone,[1] J. Mannhart[2]*

At interfaces between complex oxides, electronic systems with unusual electronic properties can be generated. We report on superconductivity in the electron gas formed at the interface between two insulating dielectric perovskite oxides, $LaAlO_3$ and $SrTiO_3$. The behavior of the electron gas is that of a two-dimensional superconductor, confined to a thin sheet at the interface. The superconducting transition temperature of ≅ 200 millikelvin provides a strict upper limit to the thickness of the superconducting layer of ≅ 10 nanometers.

Reyren et al. Science 317 (2007) 1196

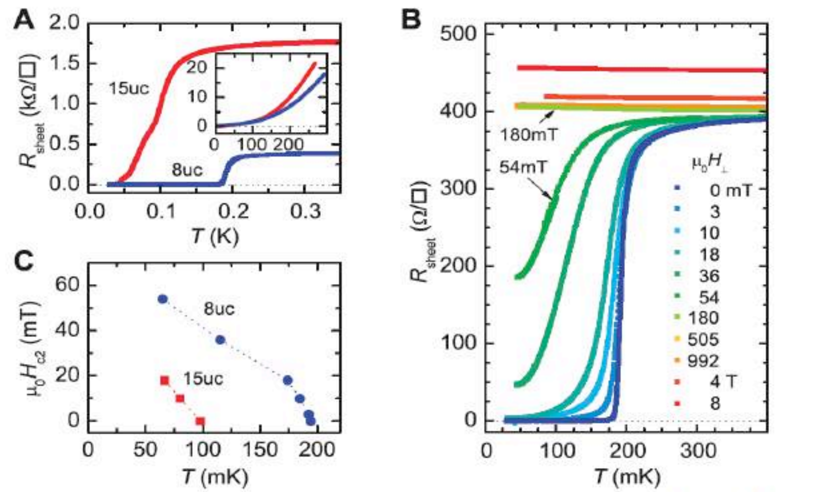

Fig. 2. Transport measurements on $LaAlO_3/SrTiO_3$ heterostructures. **(A)** Dependence of the sheet resistance on T of the 8-uc and 15-uc samples (measured with a 100-nA bias current). (Inset) Sheet resistance versus temperature measured between 4 K and 300 K. **(B)** Sheet resistance of the 8-uc sample plotted as a function of T for magnetic fields applied perpendicular to the interface. **(C)** Temperature dependence of the upper critical field H_{c2} of the two samples.

2014 Europhysics Condensed Matter prize

to Harold Hwang, Jochen Mannhart, Jean-Marc Triscone

`For the discovery and investigation of electron liquids at oxide interfaces'

Fractional Quantum Hall Effect in an Oxide 2DEG !

nature materials

LETTERS

PUBLISHED ONLINE: 17 OCTOBER 2010 | DOI: 10.1038/NMAT2874

Observation of the fractional quantum Hall effect in an oxide

A. Tsukazaki[1,2]★, S. Akasaka[3], K. Nakahara[3], Y. Ohno[4], H. Ohno[4], D. Maryenko[5], A. Ohtomo[6] and M. Kawasaki[5,7,8]★

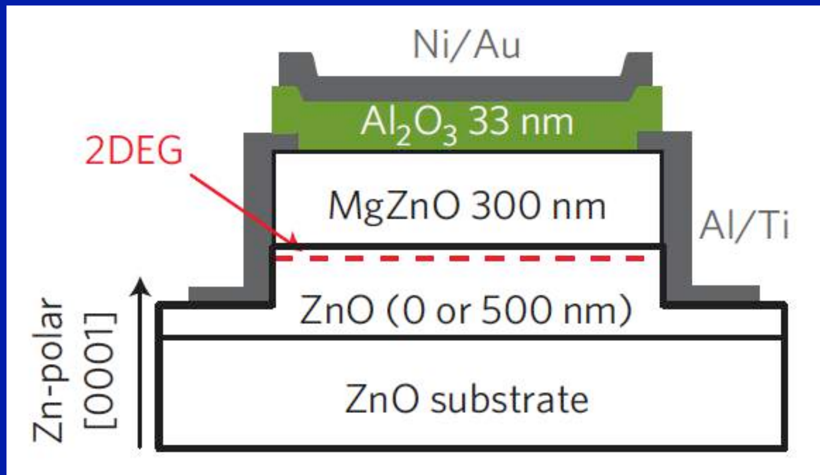

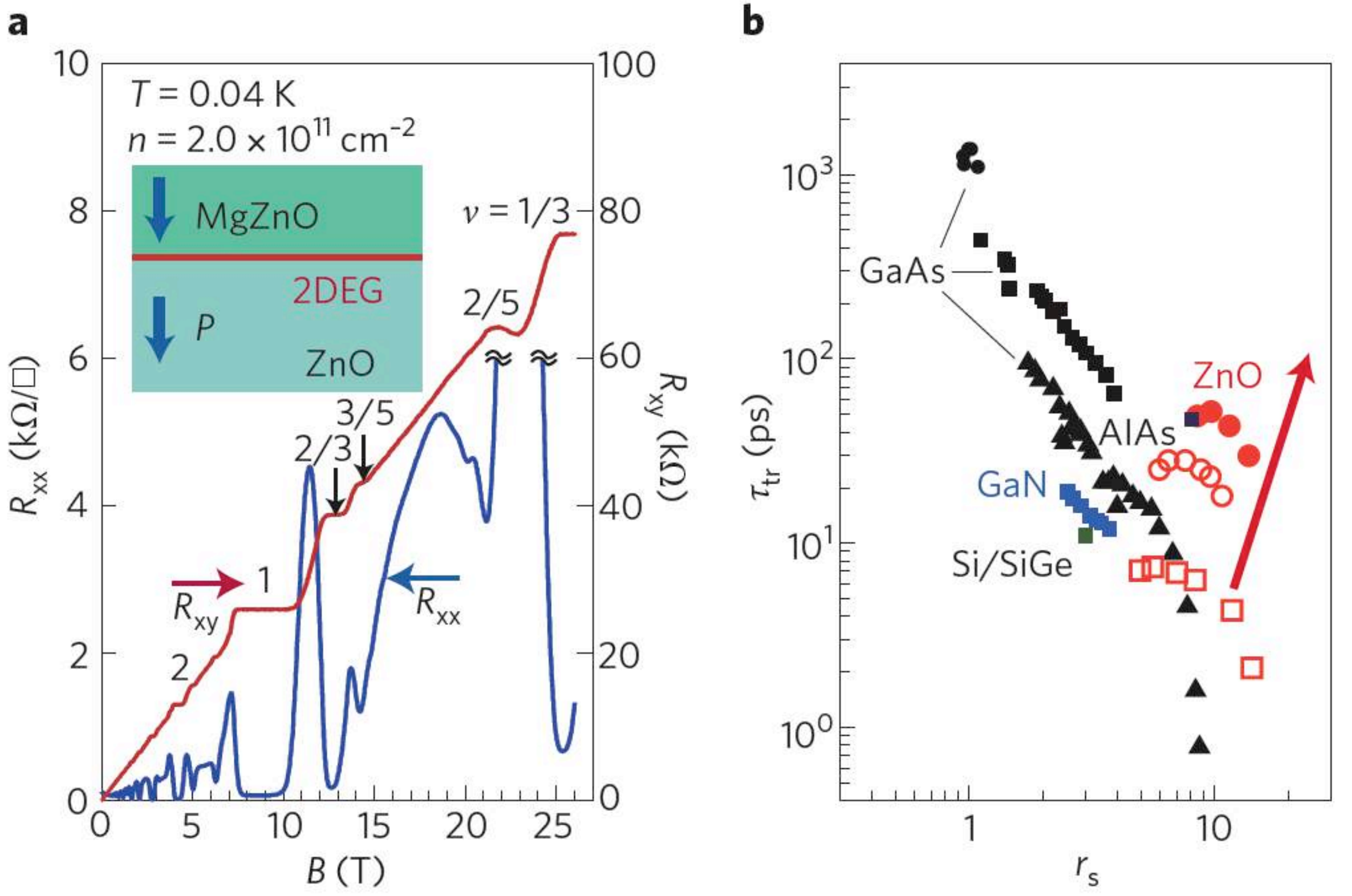

Fig from Review article Hwang et al. Nat. Mat. 11 (2012) 103

Much larger values of r_s than in conventional semiconductors, while keeping transport lifetime large enough (mobilities up to $1.8\ 10^5\ cm^2V^{-1}s^{-1}$)

Figure 8 | Fractional quantum Hall effect in ZnO. a, Longitudinal resistance R_{xx} (blue) and Hall resistance R_{xy} (red) of a 2DEG formed at a MgZnO/ZnO interface. Inset: depicts a cross-sectional schematic of the heterostructure. **b**, Comparison of 2DEGs in various semiconductors as functions of the electron–electron interaction strength represented by the Wigner–Seitz radius r_s and transport scattering time τ_{tr}. Data are derived from Fig. 2 of ref. 81 except for the solid red circles, obtained for the sample shown in **a**. The arrow indicates the direction of progress in pursuing a regime of parameters in ZnO that are hard to access in other semiconductors. Panels adapted with permission from: **a**, ref. 83, © 2011 APS; **b**, ref. 81, © 2010 NPG.

Towards applications…

- Sensitivity to external parameters:
- → Bolometers
- → Sensors
- Controllable metal-insulator transition:
- \`Piezoelectronic' transistor (PET / IBM)
- Resistive Memories (R-RAMs)
- \`\`Synaptic'' devices
- Tunable gap etc.: PV cells (e.g. $LaVO_3$)

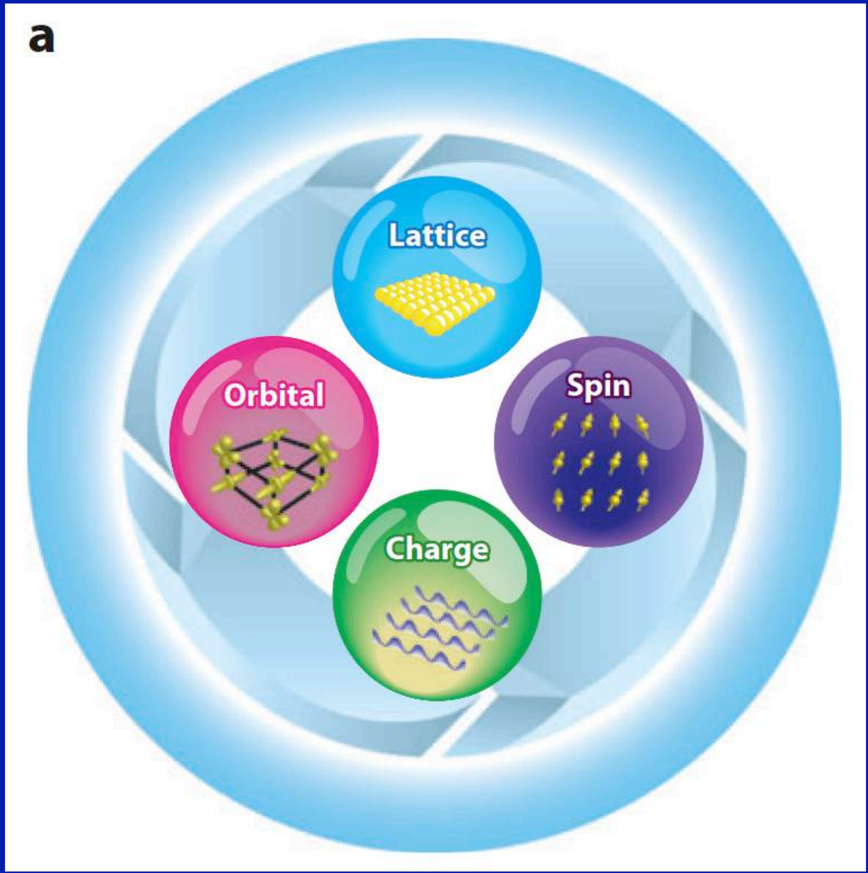

Many similar cartoons in recent review articles

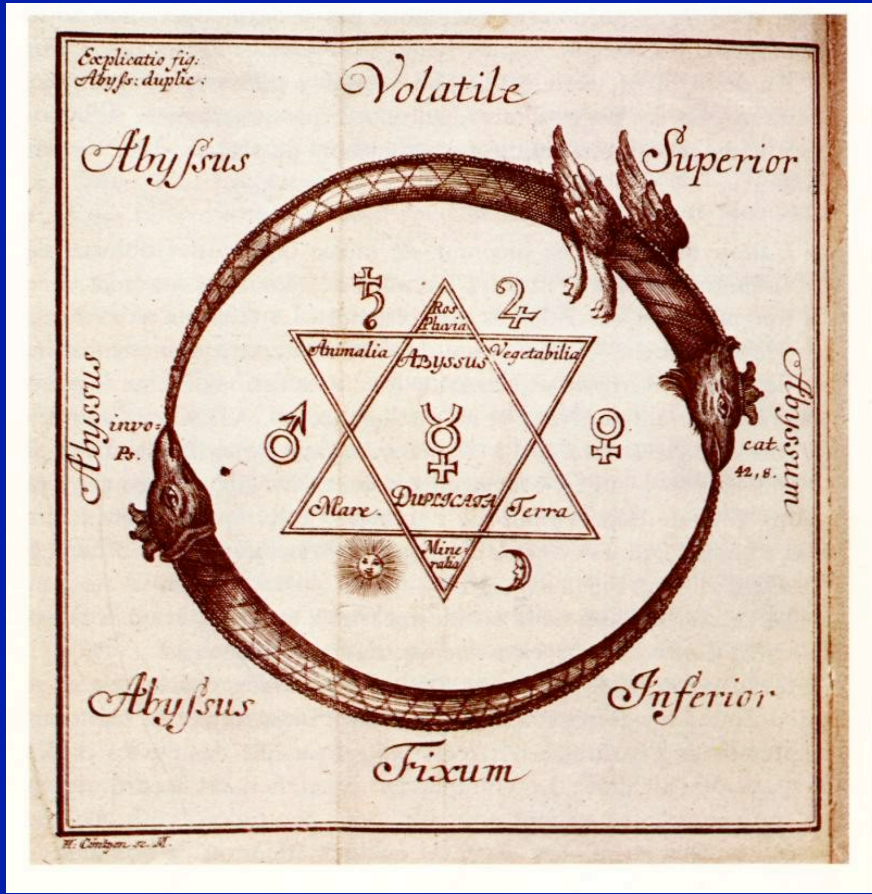

→ Quantum Materials Alchemy ?

MERCI POUR VOTRE ATTENTION !

PROCHAIN COURS:

MARDI 2 MAI 10H00